RMZ

MATERIALS and GEOENVIRONMENT

MATERIALI in GEOOKOLJE

RMZ – M&G, **Vol. 67**, No. 2
pp. 039–090 (2020)

Ljubljana, June 2020

Table of Contents
Kazalo

Historical Review

More than 90 years have passed since the University Ljubljana in Slovenia was founded in 1919. Technical fields were united in the School of Engineering that included the Geologic and Mining Division, while the Metallurgy Division was established only in 1939. Today, the Departments of Geology, Mining and Geotechnology, Materials and Metallurgy are all part of the Faculty of Natural Sciences and Engineering, University of Ljubljana.

Before World War II, the members of the Mining Section together with the Association of Yugoslav Mining and Metallurgy Engineers began to publish the summaries of their research and studies in their technical periodical Rudarski zbornik (Mining Proceedings). Three volumes of Rudarski zbornik (1937, 1938 and 1939) were published. The War interrupted the publication and it was not until 1952 that the first issue of the new journal Rudarsko-metalurški zbornik – RMZ (Mining and Metallurgy Quarterly) was published by the Division of Mining and Metallurgy, University of Ljubljana. Today, the journal is regularly published quarterly. RMZ – M&G is co-issued and co-financed by the Faculty of Natural Sciences and Engineering Ljubljana, the Institute for Mining, Geotechnology and Environment Ljubljana, and the Velenje Coal Mine. In addition, it is partly funded by the Ministry of Education, Science and Sport of Slovenia.

During the meeting of the Advisory and the Editorial Board on May 22, 1998, Rudarsko-metalurški zbornik was renamed into "RMZ – Materials and Geoenvironment (RMZ – Materiali in Geookolje)" or shortly RMZ – M&G. RMZ – M&G is managed by an advisory and international editorial board and is exchanged with other world-known periodicals. All the papers submitted to the RMZ – M&G undergoes the course of the peer-review process.

RMZ – M&G is the only scientific and professional periodical in Slovenia which has been published in the same form for 60 years. It incorporates the scientific and professional topics on geology, mining, geotechnology, materials and metallurgy. In the year 2013, the Editorial Board decided to modernize the journal's format.

A wide range of topics on geosciences are welcome to be published in the RMZ – Materials and Geoenvironment. Research results in geology, hydrogeology, mining, geotechnology, materials, metallurgy, natural and anthropogenic pollution of environment, biogeochemistry are the proposed fields of work which the journal will handle.

Editor-in-Chief

Zgodovinski pregled

Že več kot 90 let je minilo od ustanovitve Univerze v Ljubljani leta 1919. Tehnične stroke so se združile v Tehniški visoki šoli, ki sta jo sestavljala oddelka za geologijo in rudarstvo, medtem ko je bil oddelek za metalurgijo ustanovljen leta 1939. Danes oddelki za geologijo, rudarstvo in geotehnologijo ter materiale in metalurgijo delujejo v sklopu Naravoslovnotehniške fakultete Univerze v Ljubljani.

Pred 2. svetovno vojno so člani rudarske sekcije skupaj z Združenjem jugoslovanskih inženirjev rudarstva in metalurgije začeli izdajanje povzetkov njihovega raziskovalnega dela v Rudarskem zborniku. Izšli so trije letniki zbornika (1937, 1938 in 1939). Vojna je prekinila izdajanje zbornika vse do leta 1952, ko je izšel prvi letnik nove revije Rudarsko-metalurški zbornik – RMZ v izdaji odsekov za rudarstvo in metalurgijo Univerze v Ljubljani. Danes revija izhaja štirikrat letno. RMZ – M&G izdajajo in financirajo Naravoslovnotehniška fakulteta v Ljubljani, Inštitut za rudarstvo, geotehnologijo in okolje ter Premogovnik Velenje. Prav tako izdajo revije financira Ministrstvo za izobraževanje, znanost in šport.

Na seji izdajateljskega sveta in uredniškega odbora je bilo 22. maja 1998 sklenjeno, da se Rudarsko-metalurški zbornik preimenuje v RMZ – Materiali in geookolje (RMZ – Materials and Geoenvironment) ali skrajšano RMZ – M&G. Revijo RMZ – M&G upravljata izdajateljski svet in mednarodni uredniški odbor. Revija je vključena v mednarodno izmenjavo svetovno znanih publikacij. Vsi članki so podvrženi recenzijskemu postopku.

RMZ – M&G je edina strokovno-znanstvena revija v Sloveniji, ki izhaja v nespremenjeni obliki že 60 let. Združuje področja geologije, rudarstva, geotehnologije, materialov in metalurgije. Uredniški odbor je leta 2013 sklenil, da posodobi obliko revije.

Za objavo v reviji RMZ – Materiali in geookolje so dobrodošli tudi prispevki s širokega področja geoznanosti, kot so: geologija, hidrologija, rudarstvo, geotehnologija, materiali, metalurgija, onesnaževanje okolja in biokemija.

Glavni urednik

Other papers

Received: Aug 24, 2020
Accepted: Aug 24, 2020
DOI: 10.2478/rmzmag-2020-0011

In memoriam – zaslužni profesor dr. Uroš Bajželj

Professor emeritus dr. Uroš Bajželj

Quietly and suddenly, he left our world struggling with a coronavirus pandemic. Dear and respected professor emeritus dr. Uroš Bajželj unfortunately lost this battle on March 30 this year. We often look back and find that the development of any profession largely depends

Zaslužnemu profesorju dr. Urošu Bajžlju

Tiho in nenadoma je zapustil naš svet, ki se spopada s pandemijo koronavirusa. Dragi in spoštovani zaslužni profesor dr. Uroš Bajželj je to bitko žal izgubil 30. marca letos. Pogosto se oziramo nazaj in ugotavljamo, da je razvoj kate-

on the people who are committed to it and with their abilities co-shape the directions of action with a view to the future. Among them, without a doubt, we can also include the professor emeritus dr. Uroš Bajželj, to whom we sincerely thank for his contribution to the development of mining and geotechnological science.

He was born in Ljubljana on October 6th, 1931, and like many other talented children in his youth, he walked the paths dictated primarily by school and the desire for knowledge, especially in the fields of technology and science, which allowed him to be already appointed a demonstrator during his studies at the University of Ljubljana. In 1957, he successfully completed his university studies and became a graduate mining engineer. His life path first brought him to Idrija, to the Mercury Mine, where he quickly integrated into the mining environment with a centuries-old tradition and began to work systematically and creatively in the demanding professional field of mining. The hard and development-oriented work of the young engineer was highly appreciated by the employees in the mine, because he was always ready to lead development projects or participate in innovations and improvements in technical and technological processes of ore extraction in extremely complex geological conditions. Before leaving for the new position of general manager of the Kaolin and Calcite Mine Črna - Kamnik, he was the head of the development department for one year. In his new position, its ability to achieve development goals has come to the fore again, thus, in 1978, as an innovator, he was awarded the "innovation chain".

One year earlier, one of the station in his life was the position of general manager of the Mining Institute Ljubljana, where with great love and persistent work he managed to organize the institute into an internationally recognized research organization in the field of mining.

Until his election in 1987 to the title of Associate Professor of Mining at the University of Ljubljana, where he also successfully defended his doctoral dissertation, he worked scientifically and research in various fields of mining activities. Although he worked creatively in several areas of mining, his attachment to the Idrija mine never dried up. In several roles, he actively participated professionally and scien-

re koli stroke v veliki meri odvisen predvsem od ljudi, ki so ji predani in s svojimi sposobnostmi sooblikujejo smeri delovanja s pogledom naprej, v prihodnost. Mednje brez dvoma lahko štejemo tudi zaslužnega profesorja dr. Uroša Bajžlja, ki se mu na tem mestu med drugim iskreno zahvaljujemo za njegov prispevek k razvoju rudarske in geotehnološke znanosti.

Rodil se je v Ljubljani 6. oktobra 1931 leta in je kot mnogi drugi nadarjeni otroci v mladosti prehodil pota, ki jih je v prvi vrsti narekovala šola in želja po znanju, predvsem s področij tehnike in naravoslovja, kar mu je omogočilo, da je bil že v času študija na Univerzi v Ljubljani imenovan za demonstratorja. Leta 1957 je uspešno končal univerzitetni študij in postal diplomirani inženir rudarstva. Življenjska pot ga je najprej pripeljala v Idrijo, v Rudnik živega srebra, kjer se je hitro vklopil v rudarsko okolje z večstoletno tradicijo in začel sistematsko in ustvarjalno delati na zahtevnem strokovnem področju rudarstva. Naporno in razvojno naravnano delo mladega inženirja so sodelavci v rudniku visoko cenili, ker je bil vedno poleg operativnega in odgovornega dela, ki ga je opravljal kot tehnični vodja jame, pripravljen voditi razvojne projekte ali sodelovati pri inovacijah in izboljšavah tehničnih in tehnoloških postopkov pridobivanja rude v izjemno zapletenih geoloških razmerah. Pred odhodom na novo delovno mesto direktorja Rudnika kaolina in kalcita Črna – Kamnik, je bil eno leto vodja službe za razvoj. Na novem delovnem mestu je ponovno prišla do izraza njegova sposobnost udejanjanja razvojnih ciljev, tako je bil leta 1978 kot inovator nagrajen z »inovacijsko verigo«.

Eno leto prej je bila ena izmed postaj na njegovi življenjski poti delovno mesto direktorja Rudarskega inštituta Ljubljana, kjer je z veliko ljubeznijo in vztrajnim delom uspel organizirati inštitut v mednarodno prepoznavno raziskovalno organizacijo na področju rudarstva.

V času do izvolitve leta 1987 v naziv izrednega profesorja za področje rudarstva na Univerzi v Ljubljani, kjer je med drugim tudi uspešno obranil doktorsko disertacijo, je znanstveno in raziskovalno delal na različnih področjih rudarskih dejavnosti. Čeprav je ustvarjalno delal na več področjih rudarstva, njegova navezanost na idrijski rudnik ni nikoli presahnila. V več vlogah je dejavno strokovno in znanstveno so-

tifically and led projects that quided the mine through difficult periods of closure with at least partially preserved mercury production, so that he and his colleagues managed to combine environmental conditions of ore mining with adapted technological processes of precious metal extraction. The exact opposite of the centuries-old tradition of bottom-up excavation was the introduction of a top-down mining method using hardened backfill in Permo-Carboniferous shales with much lower impacts on the development of sedimentation of the narrower and wider excavation area with higher yield of native mercury, past due to its physical properties lost in the backfill below each level of excavation.

He actively led and participated in the production and implementation of mine closure projects, which were built into the mining environment in order to preserve the town of Idrija above the partially submerged cave, which for centuries gave hard-earned bread to miners and their families. As part of these mining activities, he contributed with his knowledge and rich experience to the arrangement of Antonijev rov and other mining facilities into a mining museum, which is now visited by tourists and various experts from around the world. He was also an active member of the expert commission, which oversaw the maintenance work in the wider area of the mine, throughout the closure work and later. He focused a lot of his professional and scientific potential on research for the needs of uranium ore mining in the Žirovski vrh uranium mine. Also in this "young mine" he led the development of a new mining method, with great emphasis on improved protection of miners and respect for environmental conditions, in order to guide the development of environmentally friendly mining, which at that time was not as important as today. In professional interviews and scientific debates, he indicated that he felt a special desire or a kind of mission that mining must adapt to new challenges that require economic efficiency while strictly respecting environmental requirements and ensuring the protection and health of miners who perform demanding mining works. All of this points to a mining expert and scientist, and a university teacher who had a sense of the future and a sense of realiz-

deloval in vodil projekte, ki so usmerjali rudnik skozi težka obdobja zapiranja ob vsaj delno ohranjeni proizvodnji živega srebra tako, da je uspel skupaj s svojimi sodelavci združiti okoljevarstvene pogoje odkopavanja rude s prilagojenimi tehnološkimi postopki pridobivanja dragocene kovine. Pravo nasprotje večstoletni tradiciji načina odkopavanja od spodaj navzgor je bila uvedba metode odkopavanja z uporabo utrjenega zasipa od zgoraj navzdol v permo-karbonskih skrilavcih z veliko manjšimi vplivi na razvoj posedanja ožjega in širšega območja odkopavanja ob višjem izkoristku pridobivanja samorodnega živega srebra, ki se je v preteklosti zaradi svojih fizikalnih lastnosti izgubljalo v zasipih pod vsakokratnim nivojem odkopavanja.

Aktivno je vodil in sodeloval pri izdelavi in izvajanju projektov zapiralnih del rudnika, ki so bili vgrajeni v rudarsko okolje z namenom ohranjanja mesta Idrija nad delno potopljeno jamo, ki je stoletja dajala težko zaslužen kruh rudarjem in njihovim družinam. V okviru navedenih rudarskih dejavnosti je s svojim znanjem in bogatimi izkušnjami prispeval k urejanju Antonijevega rova in drugih rudniških obratov v rudarski muzej, ki ga danes obiskujejo turisti in različni strokovnjaki s celega sveta. Prav tako je bil vseskozi, v času izvajanja zapiralnih del in kasneje, aktiven član strokovne komisije, ki je bedela nad izvajanjem vzdrževalnih del na širšem območju rudnika. Veliko svojega strokovnega in znanstvenega potenciala je usmeril v raziskave za potrebe pridobivanja uranove rude v Rudniku urana Žirovski vrh. Tudi v tem »mladem rudniku« je vodil razvoj nove odkopne metode, z velikim poudarkom na izboljšani zaščiti rudarjev in spoštovanju okoljevarstvenih pogojev, z namenom usmerjanja razvoja okolju prijaznega rudarjenja, ki v tistem času še ni bilo tako pomembno kot danes. V strokovnih razgovorih in znanstvenih debatah je nakazoval, da v sebi čuti posebno željo oziroma neke vrste poslanstvo, da se mora rudarjenje prilagajati novim izzivom, ki zahtevajo ekonomsko učinkovitost ob strogem spoštovanju okoljevarstvenih zahtev in stalnem zagotavljanju varstva in zdravja rudarjev, ki izvajajo zahtevna rudarska dela. Vse to kaže na rudarskega strokovnjaka in znanstvenika ter univerzitetnega učitelja, ki je imel občutek za prihodnost in smisel za udejanjanje

ing original ideas based on a solid professional foundation and vision. He has presented the results of research projects at numerous international conferences, symposia and congresses and lectured on research achievements at various universities around the world, including prestigious ones such as Columbia University, Henry Krumb School of Mines in New York and elsewhere.

After 1987, his work in the field of pedagogy brought him even closer to mining science. He led and organized research work in the projects with international participation in the field of introduction of hardened backfill in the metal mines and coal mines in order to ensure development of mining even in more demanding economic and environmental management conditions.

Special thanks go to him also as a leader in the establishment of the geotechnological profession in our country, which enables the transfer and application of traditional knowledge of the field of mining to the other industries and thus the existence and further development of this applied science. During his pedagogical work at the faculty, in 1993 he was elected to the title full professor of mining and geotechnology.

Under his mentorship, more than twenty students graduated, more than five of them successfully defended their master's theses and just as successfully defended their doctoral dissertations at the Department of Geotechnology, Mining and Environment at the Faculty of Natural Sciences and Engineering, University of Ljubljana.

During his tenure at the University of Ljubljana, the late Professor Uroš Bajželj performed high-quality scientific research work and other responsible functions and received several national and international awards, including the title of Honorary Doctor at Petrosani University in Romania and the title of Meritorious Member of International of the International Society of Mining Professors and the World Mining Congress - IOC-WMC. In the period 1993–1997 he was the first president of the Slovenian Mining Association of Engineers and Technicians - SRDIT and its honorary member. At the 58th Jump over the leather skin in Velenje, he received the title of honorary jumper. Until recently, he was an active member of the Slovenian Chamber of

izvirnih zamisli temelječih na trdnih strokovnih osnovah in viziji. Rezultate raziskovalnih projektov je predstavil na številnih mednarodnih konferencah, simpozijih in kongresih ter predaval o raziskovalnih dosežkih na različnih univerzah v svetu med drugimi tudi na prestižnih kot sta Columbia University, Henry Krumb School of Mines v New Yorku in drugje.

Delo na pedagoškem področju ga je po letu 1987 še bolj približalo rudarski znanosti. Vodil in organiziral je raziskovalno delo na projektih z mednarodno udeležbo s področja uvajanja utrjenih zasipov v kovinske rudnike in premogovnike z namenom zagotavljanja razvoja rudarstva tudi v zahtevnejših ekonomskih in okoljevarstvenih pogojih gospodarjenja.

Posebna zahvala mu velja kot vodilnemu pri ustanavljanju geotehnološke stroke v naši državi, ki omogoča prenose in uveljavljanje tradicionalnih znanj s področja rudarstva tudi na druge gospodarske panoge in s tem obstoj in nadaljnji razvoj te aplikativne znanstvene vede.

V času opravljanja pedagoškega dela na fakulteti, je bil leta 1993 izvoljen v naziv rednega profesorja za področje rudarstva in geotehnologije.

Pod njegovim mentorstvom je diplomiralo več kot dvajset študentk in študentov, več kot pet jih je uspešno zagovarjalo magistrska dela ter prav toliko uspešno obranilo doktorske disertacije na Oddelku za geotehnologijo, rudarstvo in okolje na Naravoslovnotehniški fakulteti Univerze v Ljubljani.

Pokojni profesor Uroš Bajželj je v času svojega delovanja na Univerzi v Ljubljani opravljal visoko kakovostno znanstveno raziskovalno delo in druge odgovorne funkcije ter prejel več domačih in mednarodnih priznanj, med katerimi velja posebej izpostaviti naslov častnega doktorja na Univerzi Petrosani v Romuniji ter podelitev naziva zaslužnega člana mednarodnih združenj International Society of Mining Professors in World Mining Congress – IOC-WMC. V obdobju 1993–1997 je bil prvi predsednik Slovenskega rudarskega društva inženirjev in tehnikov – SRDIT ter njegov častni član. Na 58. Skoku čez kožo v Velenju je prejel naziv častnega skakalca. Do zadnjega je bil aktiven član Inženirske zbornice Slovenije, ki mu je podelila pomembno nagrado za njegovo življenjsko delo na področju rudarstva in geotehnologije.

Engineers, which awarded him with award for his life's work in the field of mining and geotechnology.
Younger colleagues are proud and we will be proud of him in the future as well, even if he is no longer among us. There remains a deep respect and gratitude for all his noble deeds, which helped us in our professional decisions and other orientations in our work, which is related to the nature and difficulty of the mining profession, in its own always interesting and attractive.

Mlajši kolegi smo in bomo ponosni nanj tudi v prihodnje, čeprav ga ni več med nami. Ostaja globoko spoštovanje in zahvala za vsa plemenita dejanja, ki so nam bila v pomoč pri naših strokovnih odločitvah in drugih usmeritvah pri našem delu, ki je povezano z naravo in težavnostjo rudarskega poklica, po svoje vedno zanimivega in privlačnega.

prof. dr. Jakob Likar
izr. prof. dr. Jože Kortnik

Original scientific paper

Received: Jun 22, 2020
Accepted: Jul 10, 2020
DOI: 10.2478/rmzmag-2020-0010

Investigation of Metal-based Composites Vibration Properties Using Modal Analysis in Combination with Wavelet Transforms Under Imitation of Operational Loads

Preiskava vibracijskih lastnosti kompozitnega materiala s kovinsko osnovo z uporabo modalne analize v kombinaciji z valovno transformacijo pod imitacijo obratovalnih obremenitev

Dmitrii S. Molchanov[1,*], Heinz Palkowski[2], Sergey Chernyakin[1], Panagiotis G. Karagiannidis[3]

[1] Space Engineering Department, Samara National Research University, 34, Moskovskoye Shosse, Samara, 443086, Russia

[2] Faculty of Natural and Materials Science, Clausthal University of Technology, Agricolastraße 6, Clausthal-Zellerfeld, 38678, Germany

[3] Faculty of Technology, School of Engineering, University of Sunderland, Sunderland SR6 0DD, UK

* molchanovds63@gmail.com

Abstract

The present article is dedicated to the study of the vibration properties of metal-based composite materials and the application of the non-destructive testing method. The main modal parameters of the metal-based composites were investigated. For experimental determination of natural frequencies and modes of oscillations, the method of scanning laser Doppler vibrometry was used. For the numerical modal analysis, the finite element method was used. The material model was a layered composite with isotropic linearly elastic layers and metal layers. The task of identifying the material model was considered as the problem of minimising the discrepancy between the calculated natural frequencies and the experimental ones. The developed method can be recommended for the determination of parameters of material models for calculating the modal characteristics of polymer–metal sandwich sheets and metallic mono-materials composite products. Methodology for identifying models of elastic behaviour of polymer–metal composite materials, based on the results of the experimental modal analysis, is presented. Wavelet-based damage detection is also presented as an appropriate approach for the identification of integral conditions of the metal–polymer–metal composite

Povzetek

Predstavljen članek obravnava študijo vibracijskih lastnosti kompozitnega materiala s kovinsko osnovo in uporabo neporušitvene preiskovalne metode. V delu so bili obravnavani glavni modalni parametri kompozitnega material s kovinsko osnovo. Za eksperimentalno določitev naravnih frekvenc in načinov nihanja je bila uporabljena Dopplerjeva laserska vibrometrija. Metoda končnih elementov je bila uporabljena za numerično modalno analizo. Modelni material predstavlja plastni kompozit, ki sestoji iz izotropno linearno orientiranih elastičnih plasti in kovinskih plasti. Naloga določitve ustreznega modela sloni na rešitvi problema z minimizacijo neskladja med izračunanimi naravnimi frekvencami in eksperimentalno izmerjenimi frekvencami. Razvita metoda se lahko uporabi za določitev modelnih parametrov, predvsem za izračun modalnih lastnosti plastnih kompozitov iz polimernih in kovinskih plasti, kot tudi kovinskih mono-materialnih kompozitnih produktov. Metodologija identifikacije modelov elastičnega obnašanja polimerno-kovinskih kompozitnih materialov sloni na podlagi rezultatov eksperimentalne analize. Zaznavanje poškodb na osnovi vibracij je predstavljeno kot ustrezen pristop za prepoznavanje integralnih pogojev kompozitnih plastnih materialov

materials. Results of wavelet transform convolutions are presented.

Key words: vibration properties, laminated metal-reinforced composites, experimental modal analysis, wavelet transforms, laser vibrometry.

kovina-polimer-kovina. Predstavljeni so tudi rezultati konvolucijske valovne transformacije.

Ključne besede: vibracijske lastnosti, kompoziti ojačeni s plastjo kovine, eksperimentalna modalna analiza, valovna transformacija, laserska vibrometrija.

Introduction

Metal–polymer–metal (MPM) composites that consist of an aluminium or steel bases with oxides, nitrides or carbides reinforcements had several advantages over monolithic materials. Although in the past they were not so tough, more expensive and difficult to handle, current applications from MPMs become highly valuable. Possible applications made from these composites are interior parts, floor supports, fuselage parts, highly loaded surfaces as helicopter rotor blades, turbine fan blades, etc.

One of the current issues in using advanced composite materials in aircraft construction is to provide strength in different conditions of vibrations, typical for aviation materials. At considerable amplitudes of oscillations that can occur, for example, under resonance conditions, situations can lead to critical situations up to failure. To exclude resonance oscillations, it is necessary to calculate the modal characteristics in detail at the design stage: their natural frequencies and forms of oscillations. In the case when products made of new composite materials, this calculation is complicated by the lack of reliable data on mechanical characteristics. The main problem (in comparison with isotropic materials) is a large number of parameters to be included in the material model, as well as the fact that these parameters depend on the material layers, changing with the fibres direction, bond reinforcement and technological factors. For example, an orthotropic elastic material contains nine parameters. Their definition is a laborious task. Data on materials characteristics, given in the literature, are often contradictory, and in carrying out responsible calculations require additional verification. For the computational analysis of the stress–strain state and modal analysis structures, the finite element method (FEM) can be effectively used [1–3]. Another big issue is the control and diagnostics of such structures during operation. At present, all civil, mechanical and aerospace structures might be damaged by impacts, overloading conditions, fatigue and deterioration of material properties forced by environmental factors. Damages also place in question the ability of the structure to perform its basic functions. For these reasons, many structural systems undergo routine inspections and maintenance to ensure stable operation and extend the lifespan. Identification and further characterisation of material damages without ruining the integrity of the material are made by the means of non-destructive evaluation (NDE) or non-destructive testing (NDT) [4, 5]. For imitation of conditions that can occur during operation, cycle loading could be most appropriate. In detail, according to the test data if any stress concentrator is present, then the load that can cause failure after a certain number of cycles will be a decreasing function of these cycles. Delamination, cracks in matrix and fibres and many other irregularities can simultaneously exist in the structure. Irregularities can also influence each other and, as a result, lead to avalanche failures of the construction [6]. According to experimental data, due to uncertainties and assumptions that are inevitable in the complex application the correct FEM application requires verification and identification (adjustment) of finite element models. Under-identification of a finite element, the model should be taken a change in its parameters, which minimises the differences between the calculated and test data.

There are two main purposes of this work. The first one is the development of a methodology for identifying the parameters of the elastic behaviour, according to the results of the experimental modal analysis (EMA), by the example of the layered MPM composites. The second one is the assessment of data, acquired during the first part for evaluation of control and diagnostic method for MPM composites based on wavelet transforms.

Material and Methods

Metal-based (polyethylene/polypropylene) PP/PE core composites were used for this research. This type of MPM composites with PP/PE core is highly deformable under room temperatures. The production cost of such composites is the same as the production of the same mono-materials and approximately two times cheaper than the production of the aluminium mono-materials. High bending strength and the possibility to play with the

Table 1. *Reference samples (sandwich sheets and metallic mono-materials)*

Mono-materials				
Notation	Material	Thickness [mm]	Notation	Grade
St. 0.24	Steel	0.24	St. 0.24	TS245
St. 0.49		0.49	St. 0.49	TS245
St. 2		2.0	St. 2	NA
Sandwich				
	Thickness [mm]	Thickness [mm]	Skin	Core
RP	0.24/0.3/0.24	0.78	TS245	PP-PE
RH	0.49/0.3/0.49	1.28	TS245	
RF	0.49/0.6/0.49	1.58	TS245	
RD	0.49/2.0/0.49	2.80	TS245	
RW**	0.49/0.3/0.24	1.03	TS245	
RX***	0.49/0.3/0.24/0.3/0.24	1.57	TS245	

*Three-layered sandwich with skin sheets of 0.5 mm thickness and a 0.6 mm core layer.
**Three-layered sandwich with different thicknesses of the steel (same grade) skin sheet. The thickness of each side is given.

***Five-layered sandwich. The thickness of the outer steel sheets is given. This one should be compared with the three-layered RF due to the same metallic contribution and thicknesses but different distributions.

Table 2. *E-Moduli and Poisson's values of the mono-materials*

Mono-material	Thickness [mm]	E-Modulus [GPa]	Poisson's ratio
PP-PE	0.2/0.3/0.6	1.45	-0.45
TS 245	0.24	197	-0.247
TS 245	0.49	191	-0.276
TH 470	0.49	210	-0.264

type of energy absorption of the composite part show high potential for the implementation of such composites for industry needs (including driven and moving parts).

To enable investigating various parameters regarding the thickness ratio of the core and skin sheets of the sandwich materials as well as different mechanical properties, the following material combinations have been prepared for study. Objects of study are MPM sandwich and mono composites. Detailed information is presented in Tables 1 and 2. Similar samples are recommended by the ASTM standards for the determination of composite materials' mechanical characteristics during tension and fatigue testing [7, 8]. Samples with different thicknesses, mass and compound materials were tested. As an example, detailed results only for samples RX5L and RD1 are further presented.

Processing of the Sandwiches

The Sn-coated metal sheets used were of deep drawing quality (Tinplate® TS 245 – EU 1.0372) with thicknesses of 0.24 and 0.49 mm. The polymer was a PP/PE foil with thicknesses of 0.2, 0.3 and 0.6 mm. PP/PE represents 80% of the copolymer, and the rest 20% represents talc, rutile and barite. To produce different sandwich types, roll bonding process was used. First, the mono-materials were prepared by cleaning and

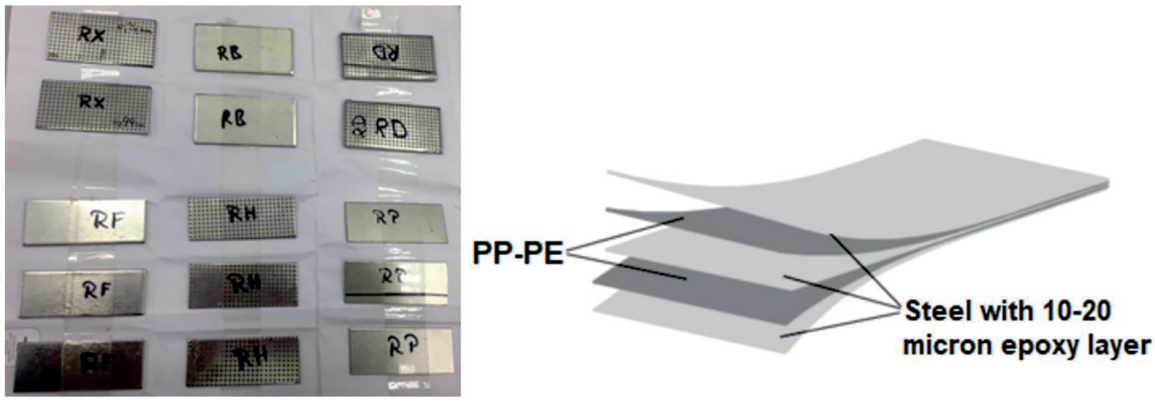

Figure 1. *Sample 'RX5L' (five-layered MPM sandwich composite; left top corner), before tests on the servo-hydraulic testing machine, and RX5L schematic structure of layers (right side figure).*

activating (polymer) and later bonded together in a two-step process using the epoxy resin Köratac FL201. The procedure is described in more detail in the study by Sokolova and others [9, 10]. For the five-layered sandwich, an additional step for preparing and activating the centre metal sheet was necessary, performing the same procedure used for the outer layers. The faultless production and quality of bonding were controlled by thermography and shear tests as described by Harhash et al. [11–13]. The Poisson's ratios of TS245 and TH470 were calculated by the width changes. Typical five-layered MPM sandwich composite among other samples is shown in Figure 1.

Theory/Calculation

The EMA is performed to obtain data about the natural frequencies and modes of oscillation, necessary for the subsequent identification of the computational model.

Modern EMA analysis, in particular, the method of scanning laser Doppler vibrometry, was used in this work. This method allows us not only to obtain high accuracy data on natural frequencies but also to determine forms of oscillations with high spatial resolution. The EMA method is based on the representation of the object under study as a vibrational system with a finite number of freedom degrees (n). The experimental determination of the natural frequencies of the system and the corresponding Eigenmodes is based on the analysis of the transfer function matrix [H], each element of which is the result of measurements of a separate frequency characteristic as the ratio:

$$H_{ij}(\omega) = \frac{X_i(\omega)}{Fj(\omega)},\ i,j = 1,\ \ldots,\ n \qquad (1)$$

where $X_i(\omega)$ is a frequency response function in the form of speed or acceleration for the i-th degree of freedom (DOF) it acts, when the $Fj(\omega)$ force corresponds to the j-th DOF and ω is the angular frequency. When using scanning laser vibrometry to one DOF of object i, an external force is applied and the response in the form of vibration velocity is measured in the set of DOF j = 1, …, n when they are sequentially scanned [14–16]. Later, according to Equation (1), the components of the transfer function matrix $H_{ij}(\omega)$ are determined. The natural frequencies are determined from the peaks on the measured amplitude–frequency response (AFR) of $H_{ij}(\omega)$. To determine their natural forms of oscillations one of the degrees of freedom is taken as the reference one, and a series of measurements of the vibration velocity amplitudes for all DOF is performed at the corresponding value of the modal frequency. The number of freedom degrees n for EMA is chosen for sufficient spatial resolution to provide a dependable presentation of the vibration modes.

The main advantage of the scanning laser vibrometry method is a non-contact measurement of vibrations, due to which the oscillation system is not exposed by additional factors

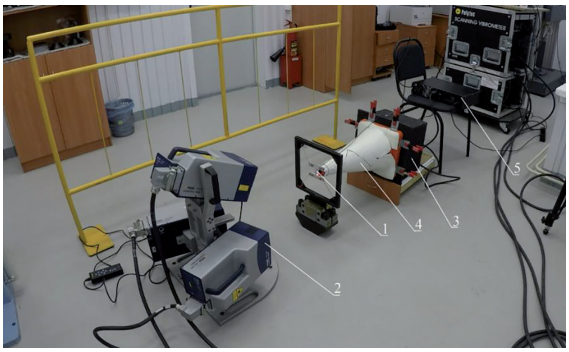

Figure 2. *Experimental facility: (1) sample, (2) three-headed laser Doppler vibrometer PSV-400, (3) acoustic oscillator, (4) acoustic diffuser and (5) amplifier.*

such as sensor masses or cable stiffnesses. It is not necessary to prepare or cut the sample or object for the test. Another advantage is the high spatial resolution: the density of the measurement points of the response is limited only by the accuracy of the laser focusing [13]. During EMA, a technique based on the Polytec PSV400-3D three-component scanning vibrometer [15–17] was used. It is a research laser-digital measuring complex, where the measurement of vibration velocity is based on the use of the Doppler effect. The PSV400-3D consists of three optical scanning laser heads, a geometry scanning module and a control system based on an industrial computer. The test sample was fixed on a rigid metal frame in compliant elastic suspensions (Figure 2).

Such scheme is often used in the EMA, which makes it possible to maximally approximate the fastening conditions to the absence of restrictions on movement ('free suspension'), convenient for reproduction in subsequent calculations. The oscillations were excited by means of specially designed acoustic dynamic. It generated a signal varying in time according to a harmonic law with a constant amplitude and a frequency (Periodic Chirp) and (White Noise) increasing to 6,000–6,400 Hz. Five experiments with different parameters of scanning net were executed for each sample. All of the tests were held in a quiet laboratory without any influential environmental noise sources. The performer started the timer to execute the experiment and left the laboratory in advance before each test. Due to the fact that vibration measured by the means of the laser Doppler vibrometer was caused by directed sound pressure in relatively small space, the influence of other minor measurement sounds in our case can be neglected.

For the calculation of modal analysis, the FEM was used. If we stated that the damping is neglected, the natural oscillations of the finite element model with (n) degrees of freedom can be described in matrix form (2).

$$[M]\left[\ddot{u}\right] + [K][u] = 0 \tag{2}$$

where $[M]$ is the mass matrix of the sample which depends primarily on its size, $[K]$ is the stiffness matrix of the sample, $[\ddot{u}]$ and $[u]$ are displacement and acceleration of the sample points, respectively. It should be noted that the stiffness matrix includes material parameters (elastic modules E and Poisson's ratios μ) and membrane and bending stiffnesses. In this case, since the sample is considered as a plate, we will have the expression for membrane stiffness in the form:

$$A = EF \tag{3}$$

where F is the cross-sectional area, and for the bending stiffness in the form:

$$D = \frac{Eh^3}{12(1-\mu^2)} \tag{4}$$

where h is the thickness of the sample.

Consequently, frequencies and waveforms will depend on both the material parameters and the sample configuration. The problem was solved by the FEM in the ANSYS Workbench software. It was assumed that the sample was free from restrictions on movement in a 'free suspension' state.

The task of identifying a material model is considered as an optimisation task with an objective function:

$$I = \sum_{i=1}^{n} a_i \left(\frac{f_{ip} - f_{ie}}{f_{ie}}\right)^2 \rightarrow min \tag{5}$$

where f_{ip} and f_{ie} are calculated and experimental values of (i) natural frequency and a_i are weight coefficients.

The control parameters are material characteristics, such as elasticity modulus and Poisson's

ratio. It is worth noting that during the manufacture of any material, researchers deal with the scatter of physical and mechanical characteristics. In particular, this means that these characteristics will change batch wise, i.e. they will be random variables. Therefore, it is impossible to guarantee that the material properties will ideally correspond to the passport data in Table 2. In addition, samples under study were made according to a certain technology. In particular, base carrier layers were rolled, and the parts of the construction were cured between each other by polymerisation process of thin epoxy layer. In this case, plastic deformation and heat treatment inevitably lead to a change in the properties of the final product.

According to the fact, that elasticity modulus, Poisson's ratio and layer thicknesses are included in the equation of vibration, i.e. they are the parameters on which the frequencies and modes of oscillations will depend. That is why, these parameters were chosen as the parameters to be optimised by Equation (5).

The weight coefficients in this equation were determined in accordance with the following approach: in the first step, for the selected *i*-th frequency, the a_i was adjusted in a way to satisfy Equation (5). The search for all frequencies here was performed independently from each other. After calculations at the first step of all a_i coefficients, their arithmetic average was found and then this coefficient was used as a weight coefficient to adjust the elastic modulus, Poisson's ratio and layer thicknesses depending on the exponent and the depending on which they enter Equation (5). At the second and at subsequent steps, the weight coefficients were selected based on a consideration of the mutual influence of frequencies on the value of Equation (5) in a way to satisfy the minimum condition of function I.

It is important that the calculated and experimental values of the natural frequencies correspond to the same own forms. In the present work, a comparison of the calculated and experimental natural (eigen) forms was carried out on the basis of an analysis of their animation representation.

For the construction of the finite element model, the finite elements of a volumetric body (SOLID185) with the option of a layered body were used. It should be noted that these elements provide modelling bulk bodies and can be used to simulate real structures. In addition, the use of the layered body option allows simulating layered bodies, in particular, composite materials. In this case, a multilayer material consists of several different materials. Special commands written in the programming language APDL (Ansys Program Design Language) set the material properties and the thickness for each layer. The finite element model of the object of study is presented in Figure 3. Table 3 presents the material characteristics and thicknesses of the layers in the sample multilayer structure which were obtained by the previously described method (Equation 5).

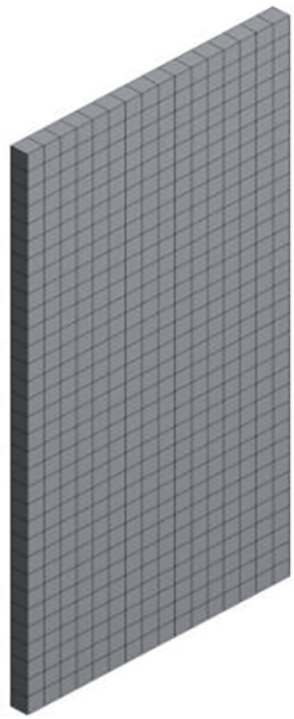

Figure 3. *Finite element model.*

Table 3. *Model parameters*

Mono-material	Thickness [mm]	E-Modulus [GPa]	Poisson's ratio
PP-PE	0.33	1.23	-0.39
TS 245	0.45/0.26	194/192	-0.245/0.3

Results and Discussion

Scattering of experimental data was estimated by the values of the coefficient of variation, which lies in the range of 0.59% (Table 4) and indicates the high accuracy of the experimental determination of the natural frequencies.

Sample vibration properties were measured (each 100,000 cycles) by means of three-headed scanning Doppler vibrometer until unstable conditions were detected. The vibration speed vector was calculated for a frequency range from 0 to 6,400 Hz. Graphs were compared.

Loading was executed by means of zero-to-tension stress cycle at the servo-hydraulic test machine SHIMADZU EHF-E (Figure 4), with the possibility of creating a wave of different shapes (sinus, triangle, straight, trapezium, 1/2 inversus, inclined plane, stepwise, arbitrary, sawtooth, oscillation, irregular) at frequencies from 10-5 to 102 Hz. In our case, we used the zero-to-tension stress cycle.

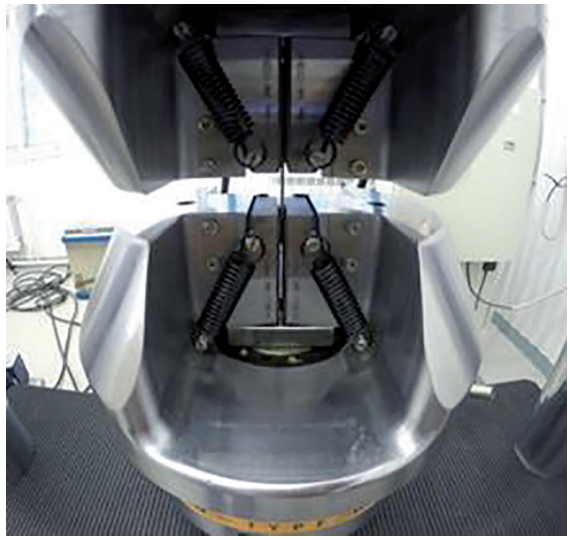

Figure 4. *Servo-hydraulic testing machine with a sample.*

Table 4. *Scattering of experimental data*

No.	Number of test/amount of scanning points					Average value	Coefficient of variation*
	1/25	2/51	3/51	4/165	5/165		
1	361	361	360	365	365	362.4	0.59
2	994	997	998	998	998	997	0.15
3	1,761	1,764	1,764	1,762	1,762	1,762.6	0.06
4	1,934	1,946	1,941	1,941	1,944	1,941.2	0.20
5	3,177	3,182	3,177	3,182	3,181	3,179.8	0.07
6	3,542	3,550	3,556	3,548	3,549	3,549	0.12
7	4,694	4,702	4,690	4,689	4,700	4,695	0.11
8	5,342	5,378	5,372	5,374	5,381	5,369.4	0.26

Note: Five experiments were carried out with various parameters of the scanning grid, which included from 25 to 165 points.

**A measure of the relative spread of a random variable, which shows that proportion of the average value is its average spread.*

Cycle loading characteristics for sample RX5L (each iteration): frequency = 80 Hz; force = 1.265 kN; cycles count = 105.

To avoid irreversible changes in the material (sample) associated with plastic deformations, the loading level was selected on the lined area of the material (stress–strain) diagram (Figure 5). Analysing the corresponding diagrams, it was concluded to select the stress load at the level of 30 MPa for all samples.

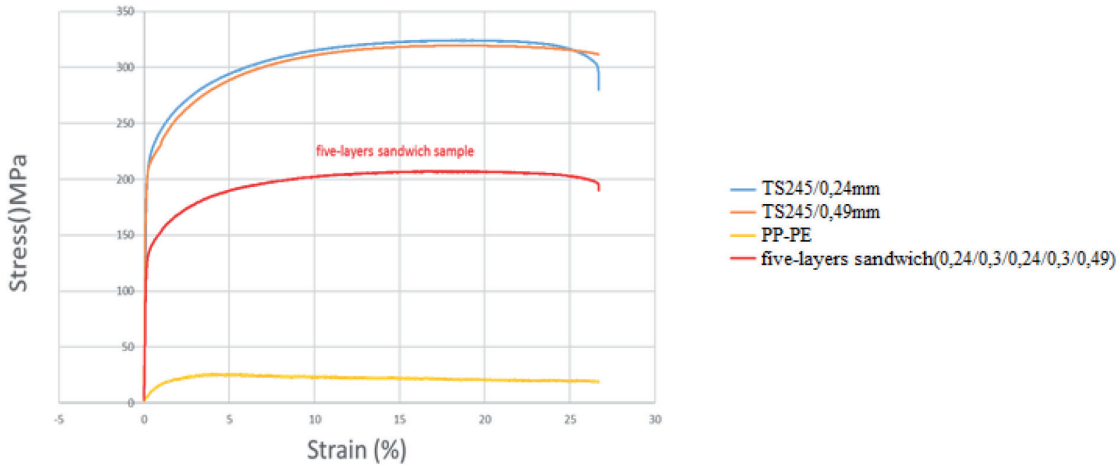

Figure 5. *Stress–strain diagrams for materials of tested samples.*

Table 5 presents the results of experimental testing (vibration vector, three heads) and computer modelling results for the five-layered sample 'RX5L'. Natural mode shapes test values and natural mode shapes FEM calculation are presented in Figures 6 and 7, respectively. The legend for FEM calculation is shown in Figure 8.

Table 5. *Test and FEM calculation values of natural modes shapes and frequencies for sample 'RX5L'*

No.	Test value		FEM calculation		Deviation [%]
	Natural mode shape (experiment)	Natural frequency [Hz]	Natural mode shape (FEM)	Natural frequency [Hz]	
1	Figure 6a	144	Figure 7a	128	12.5
2	Figure 6b	163	Figure 7b	177	7.90
3	Figure 6c	200	Figure 7c	189	5.82
4	Figure 6d	469	Figure 7d	416	12.74
5	Figure 6e	700	Figure 7e	798	12.28
6	Figure 6f	990.5	Figure 7f	1,113	11
7	Figure 6g	1,283	Figure 7g	1,441	10.96
8	Figure 6h	1,553	Figure 7h	1,480	4.93
9	Figure 6i	1,811	Figure 7i	1,732	4.56
10	Figure 6j	3,070	Figure 7j	3,503	12.36
11	Figure 6k	4,838	Figure 7k	4,365	10.83

FEM, finite element method.

Mode shapes of RX5L sample were very similar in connection with translocation on frequencies. This gives us the right to judge that the experiment was quite clear. After second and third iterations at 300,000 cycles, the graphs show small differences. After fourth iteration at 400,000 cycles, there was an obvious translocation at high-frequency ranges.

Vibration properties of 'RD1' (three-layered sandwich) sample were measured (each 100,000 cycles) by means of three-headed scanning Doppler vibrometer until unstable

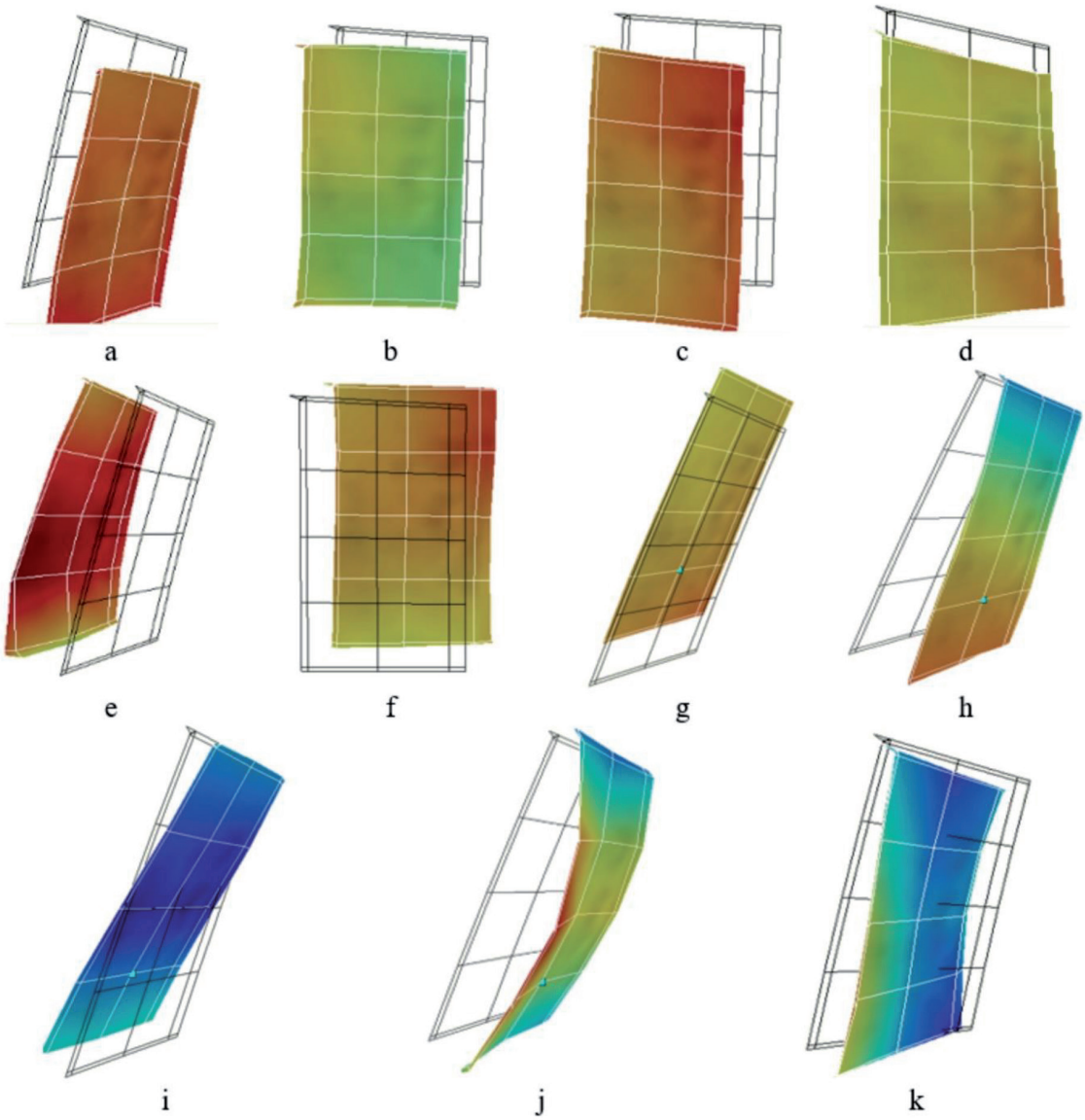

Figure 6. *Natural mode shapes: Doppler laser vibrometry experimental results.*

conditions were detected. The vibration speed vector was calculated for a frequency range from 0 to 8,000 Hz. Cycle loading characteristics (for each iteration) were: frequency = 80 Hz; force = 2.25 kN; cycles count = 100,000. Results were completely the same as with the five-layered sample, specifically the modal shapes were very familiar in connection with translocation on frequencies which also gave the confidence to judgement that the experiment was quite clear. As for RX5L sample after second and third iterations at 300,000 cycles, the graphs for the RD1 sample had small differences (in comparison with its original condition). Also after fourth iteration at 400,000 cycles, there was an obvious translocation at high-frequency ranges.

Further experiments have proved the fact that the change of vibration speed picture became enough predictable for the future forecast (Figure 9). It was found that the reference mode shapes at resonance frequencies are practically the same as with samples after 100,000–800,000 cycles loading. Another situation is with the amplitude at resonance frequencies for samples after loading of 100,000–400,000 cycles in comparison with the reference sample. Vibration speed vector

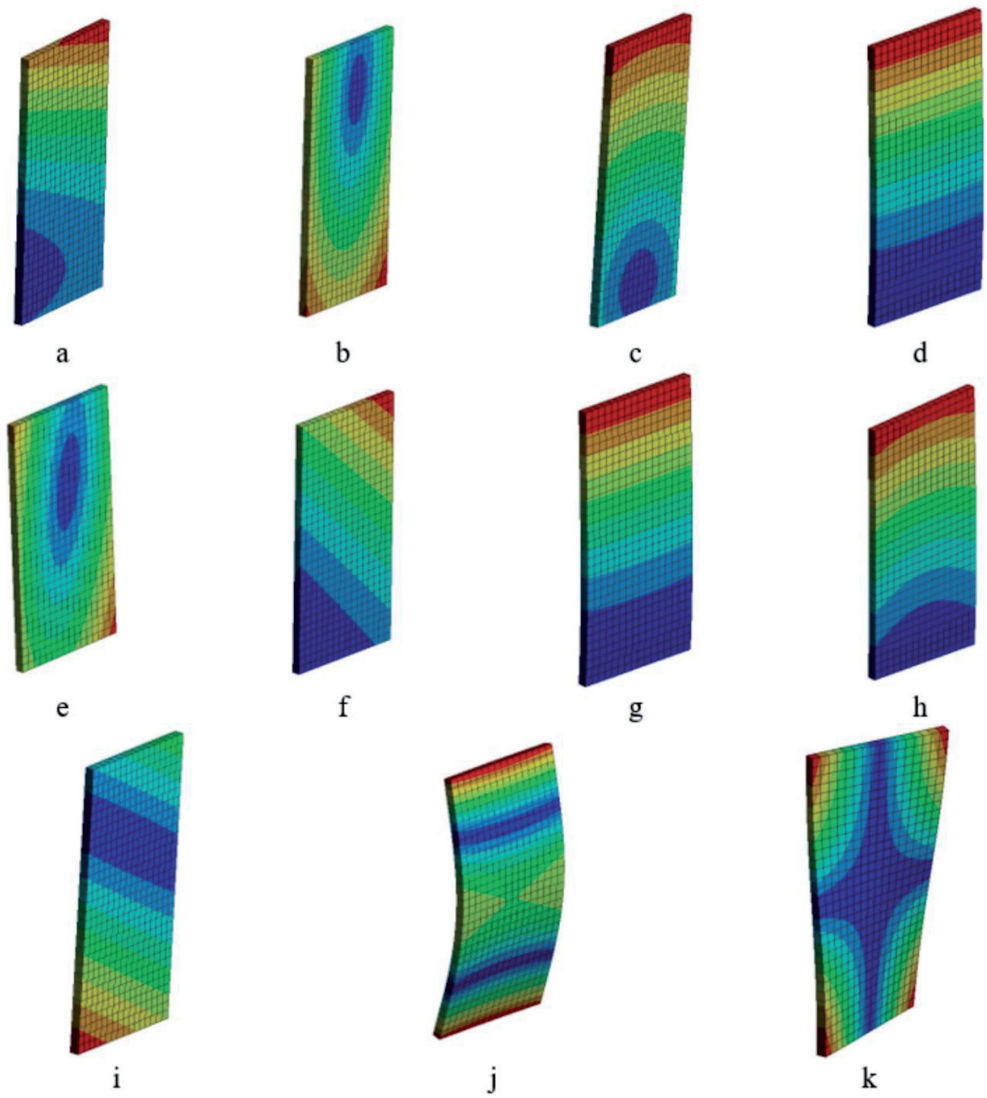

Figure 7. *Natural mode shapes: FEM calculation.*

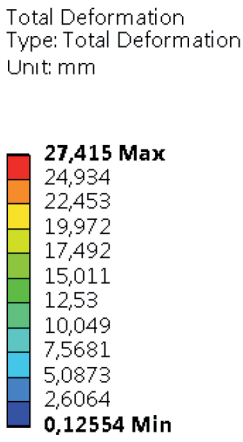

Figure 8. *Legend for finite element method calculation.*

diagrams, presented in Figure 9, shows the difference between the original and further conditions. There is an increase in the amplitude at low frequencies of approximately 30% and a sharp increase in the amplitude at frequencies above 500 Hz (equal to more than 100% of the amplitudes of the original samples at the same frequencies).

This research indicates that wavelet-based NDE analysis could provide a basis for determining damage levels in structural composite aerospace components, and thus being a means to decide whether a component is still operational. It is worth mentioning that the transformed signal reflects the overall picture of registered

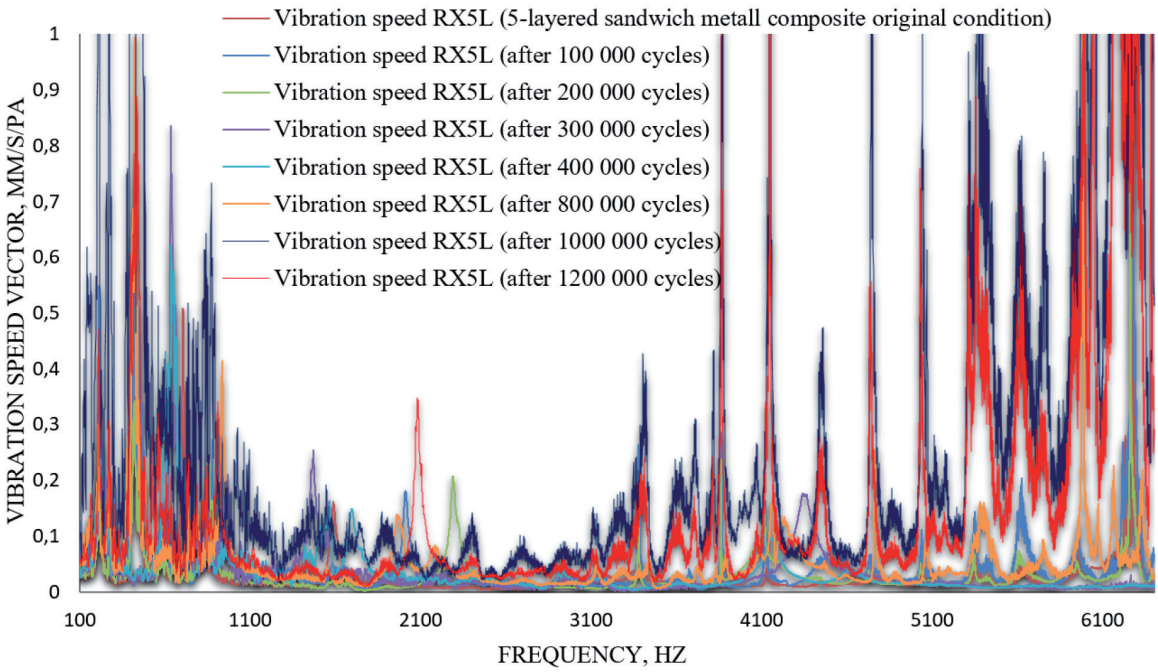

Figure 9. *'RX5L' (five-layered sandwich) vibration speed vector–frequency diagram.*

vibration. Briefly, wavelets are functions that can be applied to the signal function to search for different deviations. Opposite to Fourier transforms that can give information mostly at frequency domain, wavelet transforms allow getting information both at frequency and time domains. The transformed signal can be presented as three-dimensional (3D) plot of amplitude as a function of scale and translation. In our case, constant translation with variation only on scale parameter was accomplished. Additional basic theory information on wavelets can be found in the study by Molchanov and others [19, 20].

Based on the proposed algorithm, Fourier transformation is separately used for the determination of certain frequencies and resonance picture evaluation. Only the combination of these techniques can give affordable information for the interpretation of the obtained results. The same behaviour of vibration speed vector functions can be seen with all tested samples. It should also be mentioned that stress–strain diagrams were checked during each iteration (see Figures 10 and 11). It should be mentioned that by the value of the hysteresis loop space, we can also estimate the work spend on damage accumulation (the lower the space, the lower the work).

Experiments were executed until critical conditions. As an example, a five-layered sample was broken after 1,263,200 cycles. Stress–strain diagram at 63,200 cycles (seven load iteration for RX5L sample) is presented in Figure 12.

The second part of the article is devoted to the simplified method of obtaining amplitude response in combination with using Fourier and wavelet transforms. Additional detailed and basic information on the used method of wavelet transforms and data on vibration diagnostic signs acquired in previous works can be found in Molchanov and others [18, 19].

The presented experimental facility contains almost the same equipment (Figure 13). The main difference is the use of a one-headed laser Doppler vibrometer PDV-100, USB-4431 sound and vibration device and average processing capacity notebook. USB-4431 (102.4 kS/s, 100 dB, 0.8 Hz AC/DC coupled, 4-Input/1-Output Sound and Vibration Device) designed for sound and vibration measurements. Input channels incorporate integrated electronic piezoelectric (IEPE) signal conditioning for accelerometers and microphones. The four

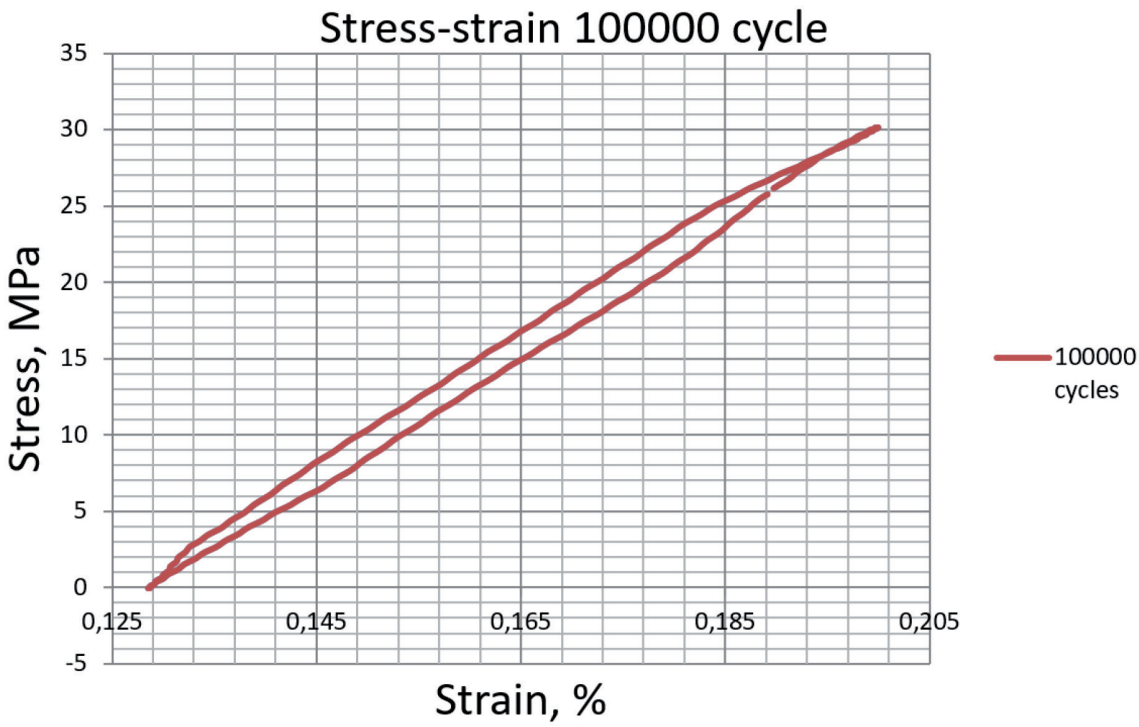

Figure 10. *Stress–strain 100,000 cycles for sample 'RX5L' (five-layered sandwich).*

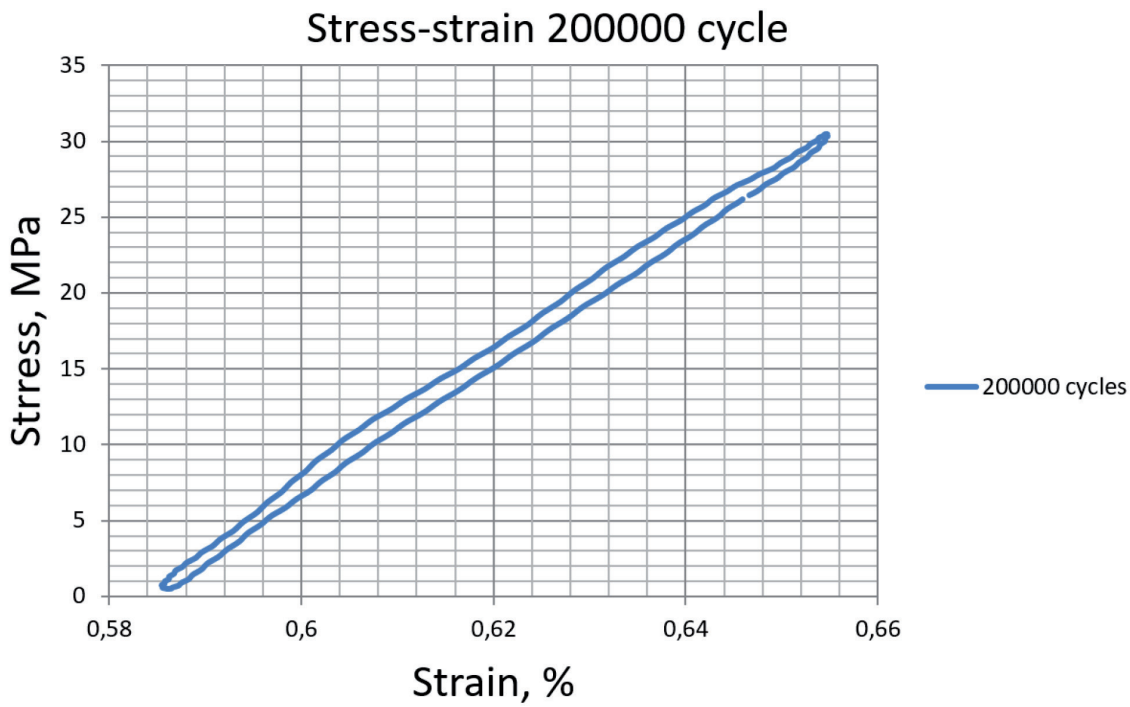

Figure 11. *Stress–strain 200,000 cycles for a sample 'RX5L' (five-layered sandwich).*

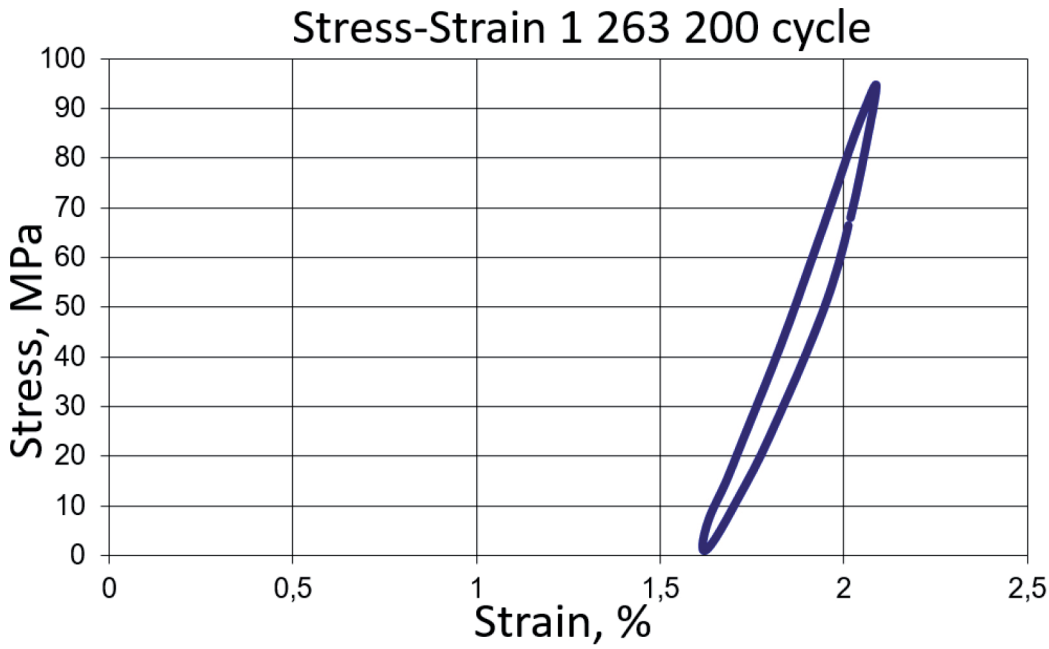

Figure 12. *Stress–strain diagram for a sample 'RX5L' (five-layered sandwich) during the break.*

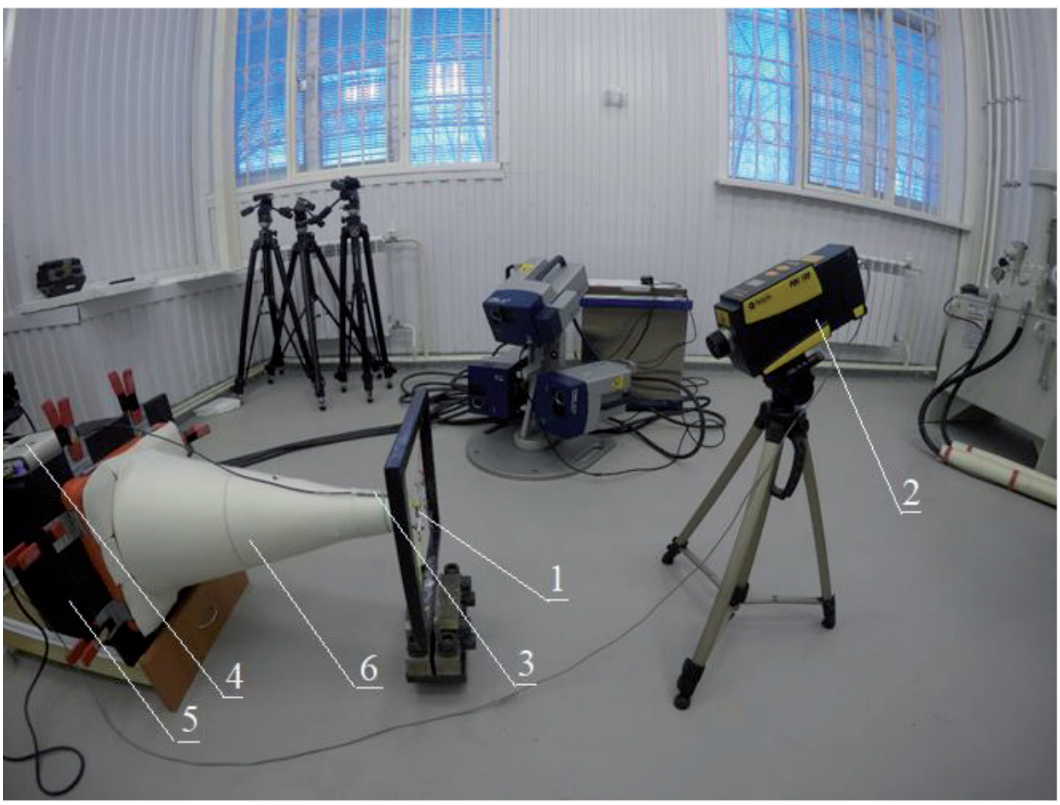

Figure 13. *Experimental facility: (1) sample, (2) one-headed laser Doppler vibrometer PDV-100, (3) microphone, (4) NI-USB-4431, (5) acoustic oscillator and (6) acoustic diffuser.*

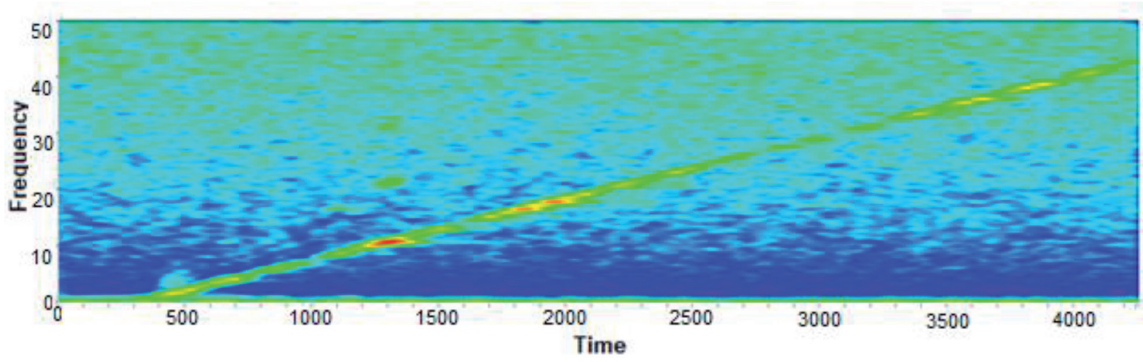

Figure 14. *Spectrogram of the reference sample RD1.*

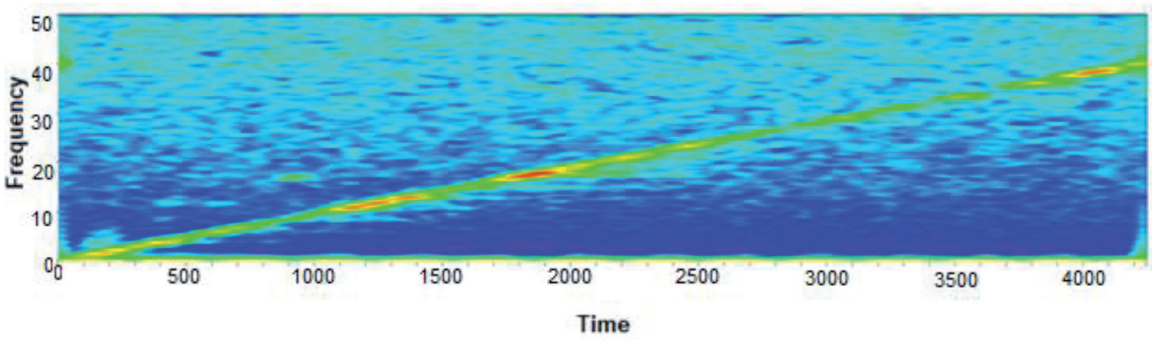

Figure 15. *Spectrogram of the sample RD1 after 100,000 cycles.*

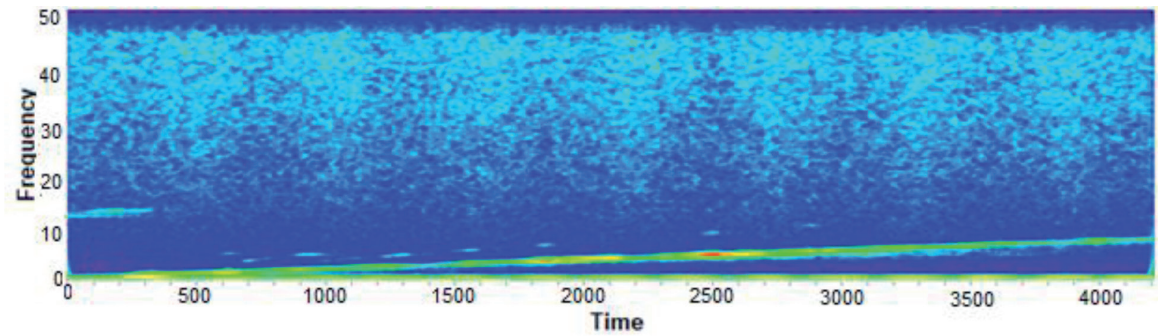

Figure 16. *Spectrogram of the sample RD1 after 300,000 cycles.*

USB-4431 input channels simultaneously digitise input signals. The analogue output (AO) channel is ideal for stimulus-response tests and it can be synchronised to the AI channels. After the measurement, recorded signals were put into written LabVIEW (Laboratory Virtual Instrumentation Engineering Workbench) program for calculation of Fourier spectrograms and wavelet transform convolutions. Another difference is the use of periodic chirp as generated sound in opposite to the white noise sound used in the first experimental part.

Results for the RD1 sample as spectrograms and 3D scalogram reflection after periodic chirp excitation (using one laser head) are presented in Figures 14–16. Signs of deterioration of the structure are natural frequency decline, damping of high frequencies, amplitude increase on a small scale, an increase in intensity at low frequencies, relevant frequencies 'Drift', the shift

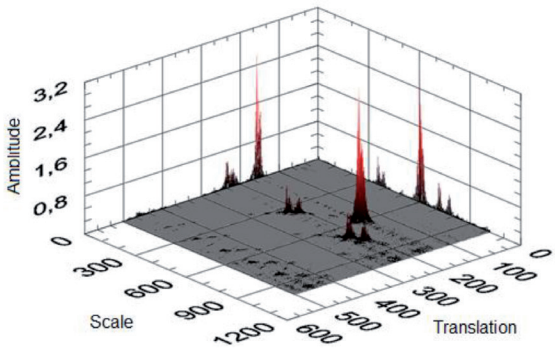

Figure 17. *Signals of sample RD1 after wavelet convolution (mother wavelet db02; scale 1024).*

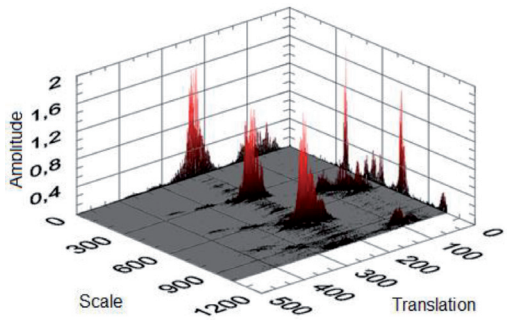

Figure 19. *The signal after wavelet convolution (mother wavelet db02; scale 1024). Sample RD1 after 200,000 cycles.*

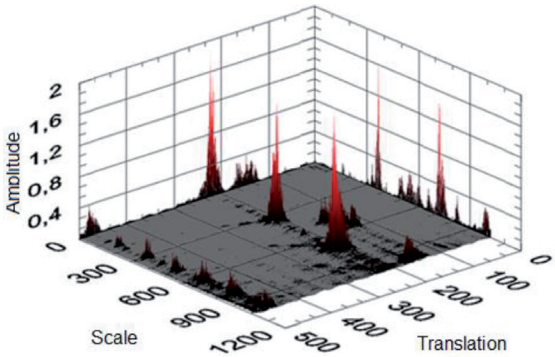

Figure 18. *The signal after wavelet convolution (mother wavelet db02; scale 1024). Sample RD1 after 100,000 cycles.*

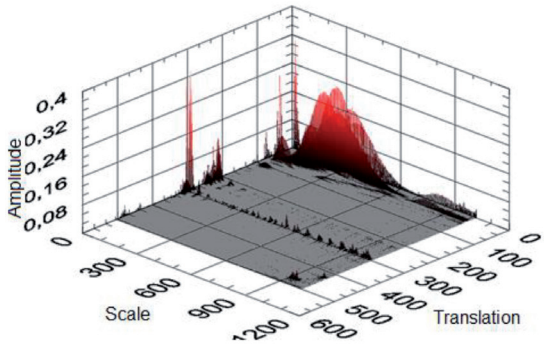

Figure 20. *The signal after wavelet convolution (used mother wavelet db02; scale 1024). Sample RD1 after 300,000 cycles.*

of the continuous wavelet transform (CWT) maximum towards larger scale (towards lower frequencies), low amplitude and absence of high frequencies (high frequencies could not be generated).

From the spectrum, it can be seen that a conventional sample spectrogram has higher values of vibration velocity than spectrograms after 100,000 and 300,000 cycles. Despite lower amplitude rise in time in comparison with the previous state, the increasing subharmonic activity with cycle load after each iteration can be seen. That is a direct sign that during use a more rapid failure under high vibration conditions is possible.

Visual features of 3D scalograms indicate changes in the overall vibration picture of the signal, which can describe the integral damage condition of the object itself. The wavelet transformed the function of the reference sample and it is presented in Figure 17. Further results are presented in Figures 18–20, respectively.

Signs of deterioration of the structure are natural frequency decline, damping of high frequencies, amplitude increase on a small scale, an increase in intensity at low frequencies, relevant frequencies 'Drift', a shift of the CWT maximum, overall low amplitude, absence of high frequencies (high frequencies could not be generated). With the increase of cycle loading after each iteration, the CWT picture changes strongly. This allows us to make a conclusion about typical signs occurring from 3D scalograms.

It is obvious that for each object the picture will be different, but there are changes that can be marked during the life cycle (as an example) to set the points in operation for maintenance checks. If the data can be collected statistically by means of many iterations (vibration tests) during operation and such deviations in connection with other parameters like resonance frequencies, this could give a reliable data on condition picture of the researchable object. Studies by Swiderski and his colleague [21, 22]

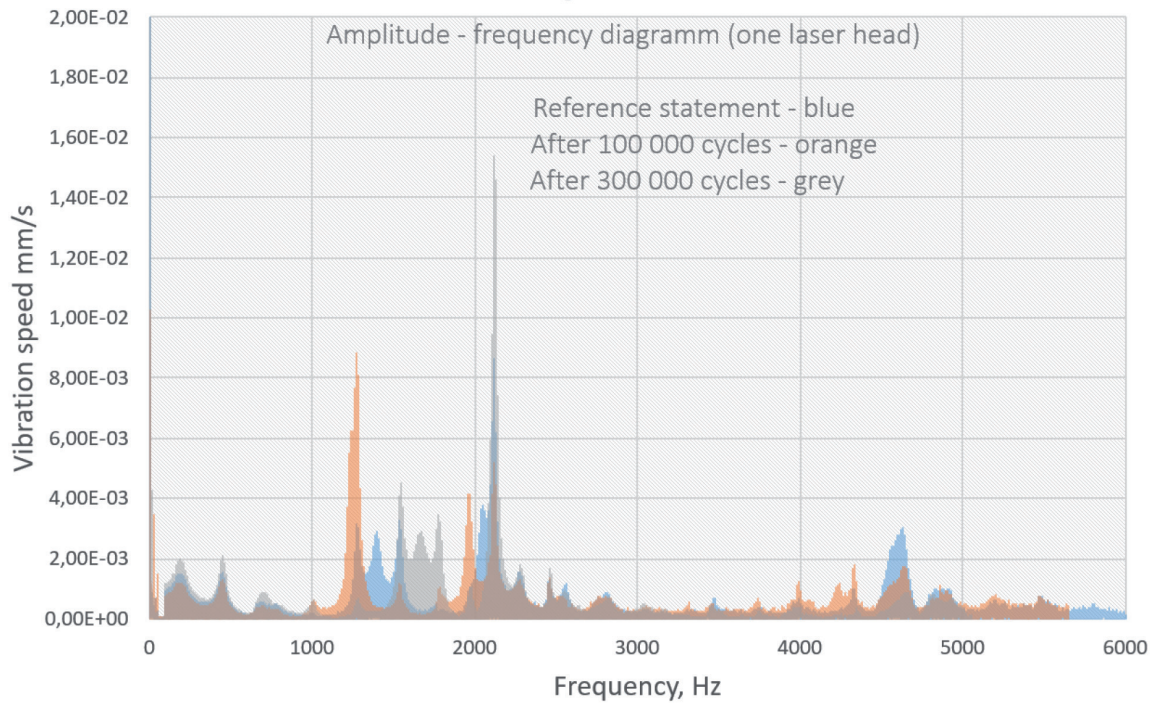

Figure 21. *Amplitude–frequency diagram. RD1 sample reference statement and after 100,000 and 300,000 cycles (one-headed Doppler laser vibrometer).*

contain additional information about experimental investigations of defect sizing in composite materials and different inverse and direct measurement problems.

The amplitude–frequency diagram (Figure 21) contains a comparison of data in the original condition and after 100,000 and 300,000 cycles for RD1. This diagram that was acquired at more simple equipment (by the means of one laser) also shows the tendency, when amplitude on certain frequencies changes according to forecast. It should be mentioned that vibration speed at frequencies close to 20–80 Hz was up to 0.06 mm/s (after 300,000 cycles), and the fact that amplitude growth at this low-frequency range was connected with cyclic loading.

Conclusion

During the calculation of modal characteristics (natural frequencies and vibration modes) of products made of polymer composite materials, it is necessary to exclude their resonance oscillations that requires reliable data on the mechanical characteristics of the material. The problem is a large (in comparison with isotropic materials) quantity of elasticity characteristics, and also in the fact that these parameters depend on a wide range of structural and technological factors.

One of this work purposes was to develop a methodology for identifying models of elastic behaviour of polymer–metal composite materials based on the results of the EMA. The object of investigation was layered reinforced sandwich sheets and metallic mono-materials.

The method of scanning laser vibrometry is used for experimental determination of natural frequencies and modes of oscillations. For the numerical modal analysis, the FEM is used. The material model is a layered composite with isotropic linearly elastic layers and metal layers. The task of identifying the material model is considered as the problem of minimising the discrepancy between the calculated natural frequencies and the experimental ones. To solve it, the quasi-random search method is used. The developed method can be recommended for the determination of parameters of material models for calculating the modal characteris-

tics of polymer–metal sandwich sheets and metallic mono-materials composite products.

For the EMA, a three-scanning and optimised one-scanning laser vibrometer were used; with its help, this work succeeded in obtaining semi-natural oscillation frequencies of samples, made from the metal composites in a frequency range up to 6,000 Hz with very insignificant scattering (overall average within 0.59%), and own forms with high space resolution.

Observation of the behaviour of five-layered samples under increasing of the load parameters led to the following conclusions. (1) The percentage ratio of certain material dictates its behaviour. Otherwise speaking, more percentage of the metal inside the construction shows more metal behaviour of the MPM composite as homogeneous substance. The opposite is true as well – more polymer shows more inhomogeneous behaviour. (2) Based on the experience with composite blades, it can be declared that for this type of MPM composites, significant amplitude increase at average frequency spectrum in combination with high damping of all other frequencies in the range from approximately 1,180 up to 3,050 Hz can be used as a diagnostic sign of unstable operation condition of the structure.

Similar to previous works with different elements made of composite material, obvious signs of alteration in CWTs were detected. The same features such as virtually unchangeable mode shapes at resonant frequencies after long cycle loading, natural frequency declines, damping of frequencies, amplitude increase on a small scale, an increase in intensity at low frequencies, shift of the CWT maximum, overall low amplitude were detected. According to tests and modelling procedures provided, metal-based composites are not an exception in behaviour. This research also indicates that wavelet-based NDE analysis in combination with complex modal analysis could provide a basis for determining damage levels in structural composite components, and thus a means to decide whether a component is still operational.

Acknowledgements

We gratefully thank for the financial support of the investigation within the project PA 873/42-1, financed by the DFG (German Research Community) and support of the Ministry of Education and Science of the Russian Federation. Moreover, we thank ThyssenKruppNirosta GmbH for delivering the metal sheets.

References

[1] Leontev, N.V. (2006): *Application of the ANSYS system to solving modal and harmonic analysis problems.* Nizhniy Novgorod Government University: Nizhniy Novgorod, 101 p.

[2] Laxalde, D., Thouverez, F., Sinou, J.J., Lombard, J.P., Baumhauer, S. (2007): Mistuning identification and model updating of an industrial blisk. *International Journal of Rotating Machinery*, vol. 2007, pp. 1–10, DOI: 10.1155/2007/17289.

[3] Grinev, M.A., Anoshkin, A.N., Pisarev, P.V., Shipunov, G.S., Nikhamkin, M.Sh, Balakirev, A.A., Konev, I.P., Golovkin, A.A. (2016): Calculation and experimental studies of the natural frequencies and vibration modes of the blade of a rectifying apparatus made from polymer composite materials. *PNRPU Mechanics Bulletin,* 4, pp. 106–119.

[4] Staszewkij, W., Boller, C., Tonlinson, G. (2004): *Health monitoring of aerospace structures*. John Wiley & Sons: West Sussex.

[5] Blanas, P., Das-Gupta, D.K. (2000): Composite piezoelectric materials for health monitoring of composite structures. In: *Materials Research Society Symposium - Proceedings*, Boston, Uchino, K., Ito, Y. (ed.). Cambridge University Press: Pennsylvania, pp. 45–50.

[6] Kassapoglou, C. (2012): *Predicting the structural performance of composite structures under cyclic loading*. Ph.D. Thesis. Harvard University, Faculty of Aerospace Engineering, Department of Aerospace Structures and Computational Mechanics: Cambridge, 140 p.

[7] Karabutov, A.A., Murashov, V.V., Podymova, N.B., Oraevsky, A.A. (1998): Nondestructive characterization of layered composite materials with a laser optoacoustic sensor. In: *Proceedings of Society of Photo-Optical Instrumentation Engineers*, Doctor, S.R., Nove, C.A., Daaklini, G.Y. (eds.). Society of Photo Optical, pp. 103–111.

[8] Kolodii, B.I., Lyaschuk, O.B. (1995): Direct and inverse problems of electromagnetic diagnostics of flat-laminated composite materials with the use of a rectangular waveguide. *Materials Science*, 30(2), pp. 173–181.

[9] Sokolova, O., Carradó, A., Palkowski, H. (2010): Production of customized high-strength hybrid sandwich structures. *Advanced Materials Research*, 137, pp. 81–128.

[10] Sokolova, O. (2012): *Study of metal/polymer/metal hybrid sandwich composites for the automotive industry.* Papierflieger, 160 p.

[11] Harhash, M., Carradò, A., Palkowski, H. (2016): Deep- and Stretch-Forming of Steel/Polymer/Steel Laminates. In: *2. International Conference. "Euro Hybrid Materials & Structures"*, Hausmann, J., Siebert, M. (eds.). p. 69–74.

[12] Harhash, M., Carradò, A., Palkowski, H. (2016). Forming Potential of Low-Density Laminates. In: *Proceedings of Euro Hybrid Materials and Structures*, Hausmann, J.M., Siebert, M. (eds.). DGM: Stade, pp. 53–60.

[13] Harhash, M., Palkowski, H., Carrado, A. (2017): *Forming behaviour of multilayer metal/polymer/metal systems.* Technische Universität Clausthal: Clausthal, 186 p.

[14] Heylen, W., Lamens, S., Sas, P. (2003): *Modal analyses. Theory and testing*. Katholieke Universiteit Leuven: Leuven, 325 p.

[15] Vibration measurements of the aerospace industry [online]. Polytec, renewed 1/01/2020 [cited 1/15/2020]. Available on: *http://www.polytec.com*.

[16] Inozemtsev, A.A., Nikhamkin, M.Sh., Voronov, L.V., Gladkiy, I.L., Golovkin, A. Yu., Bolotov, B.P. (2010): Experimental and calculated modal analysis of fan blades of hollow structure. *Aviatsionnaya promyshlennost*, 3, pp. 8–11.

[17] Grinev, M.A., Anoshkin, A.N., Pisarev, P.V., Zuyko, V.Yu., Shipunov, G.S. (2015): Computer modeling of the mechanical behavior of a composite blade of an aircraft engine straightener. *PNRPU Mechanics Bulletin*, 3, pp. 38–51.

[18] Molchanov, D.S., Makaryants, G.M., Safin, A.I., (2017): Defect-caused alteration of a composite unit modal parameters. *Measurement: Journal of the International Measurement Confederatio,* 95, pp. 383–388, DOI: 10.1016/j.measurement.2016.10.011.

[19] Molchanov, D., Safin, A., Luhyna, N., (2016): Damage monitoring of aircraft structures made of composite materials using wavelet transforms. *IOP Conference Series: Materials Science and Engineering,* 153(1), pp. 1–9, DOI:10.1088/1757-899X/153/1/01.2016.

[20] Daubechies, I. (1992): *Ten lectures on wavelets*. Mathematics: Philadelphia, 341 p.

[21] Swiderski, W., Szudrowicz, M. (2014): Experimental investigations of defect sizing in composite materials by ir thermography methods. In: *Proceedings of the 16th European Conference On Composite Materials*, European Conference on Composite Materials, pp. 1–8.

[22] Swiderski, W. (2003): Lock-in thermography to rapid evaluation of destruction area in composite materials used in military applications. In: *Proceedings of SPIE - The International Society for Optical Engineering,* Tobin, Jr.K.W., Meriaudeau, F. (eds.). Society for Optical Engineering: Gatlinburg, pp. 506–517.

Original scientific paper

Received: Mar 20, 2020
Accepted: May 18, 2020
DOI: 10.2478/rmzmag-2020-0007

Effect of Temperature and Time on Decomposition of δ-ferrite in Austenitic Stainless Steel

Vpliv temperature in časa na razpad delta ferita v avstenitnem nerjavnem jeklu

Almaida Gigović-Gekić*, Hasan Avdušinović, Amna Hodžić, Ermina Mandžuka
Faculty of Metallurgy and Technology, University of Zenica, Bosnia and Herzegovina
* almaida.gigovic-gekic@mtf.unze.ba

Abstract

Microstructure of austenitic stainless steel is primarily monophasic, i.e. austenitic. However, precipitation of the δ-ferrite in the austenite matrix is possible depending on the chemical composition of steel. δ-Ferrite is stable on room temperature but it transforms into σ-phase, carbides and austenite during heat treatment. In this work, the results of analysis of influence of temperature and time on decomposition of δ-ferrite are presented. Magnetic induction method, microstructure and hardness analyses were used for testing the degree of decomposition of the δ-ferrite. Analysis of results showed that increase in temperature and time increases the degree of decomposition of δ-ferrite.

Keywords: austenitic stainless steel, δ-ferrite, σ-phase, carbides, hardness.

Povzetek

Mikrostruktura avstenitnega nerjavnega jekla je enofazna, tj. avstenitna. Kljub temu, pa je v odvisnosti od kemijske sestave jekla mogoča tudi prisotnost delta ferita v avstenitni osnovi. Delta ferit, ki je obstojen pri sobni temperaturi, med toplotno obdelavo razpade v sigma fazo, karbide in avstenit. V tej raziskavi so predstavljeni rezultati vpliva temperature in časa na razpad delta ferita. Za izračun stopnje razpada delta ferita je bila uporabljena magnetna indukcijska metoda in analiza mikrostrukture ter trdote. Analiza rezultatov je pokazala, da se stopnja razpada delta ferita poviša s temperaturo in časom.

Ključne besede: avstenitno nerjavno jeklo, delta ferit, sigma faza, karbidi, trdota.

Introduction

Formation of the δ-ferrite is possible by solidifying or welding austenitic stainless steel and it is stable on room temperature. Depending on the chemical composition of the contents of the δ-ferrite stabilising elements such as Cr, Si, Ti, Mo, etc., the solidification can start with the crystallisation of austenite or δ-ferrite [1]. Austenitic stainless steel can be solidified in four modes, namely austenite, austenite–ferrite, ferrite–austenite and ferrite. Mode of solidification is very important because it influences the properties of steel, especially mechanical properties and welding ability. Cryogenic toughness and high temperature embrittlement are strongly influenced by the presence of δ-ferrite [2, 3]. δ-Ferrite is ductile at room and high temperatures but brittle at cryogenic temperatures. Presence of the δ-ferrite in austenitic Cr-Ni steel and in welded joints increases its strength properties, since grain growth is slowed by the volume-centred cubic crystal structure, and also by the fact that the interfacial boundaries present stronger barriers to the dislocation than the single-phase grain boundaries. However, the δ-ferrite plays a very important role in welding of austenitic stainless steel because it prevents the formation of hot cracks. So it is recommended that up to 10% of δ-ferrite should be present in weld metal. Also, precipitation of intermetallic phase is increased in the presence of δ-ferrite. Depending on the temperature of the heat treatment, the δ-ferrite can be transformed into σ-phase, carbides (type $M_{23}C_6$) and austenite [3–7]. With regard to austenite, the δ-ferrite remains a chromium-rich area where diffusion of chromium and other alphagenic elements is faster. Therefore, δ-ferrite is a suitable place for σ-phase precipitation. The σ-phase is hard and brittle and it increases the hardness while decreasing the toughness and elongation of the steel. Also, as a result of increasing the content of the s phase, the type of fracture changes from transcrystalline to intercrystalline [8]. During the heat treatment or welding, the occurrence of carbides usually precedes the appearance of intermetallic phases. $M_{23}C_6$ carbides usually form first at grain boundaries and twin boundaries and then into the austenitic matrix. Carbides precipitated on grain boundaries particularly make worst the impact properties similar to the corrosion behaviour of austenitic stainless steel [9, 10]. Due to its very high temperature, it is useful to know the microstructure behaviour of austenitic stainless steel because the mechanical and other properties depend on it. Also, it is possible to have the δ-ferrite in austenitic microstructure, especially during welding, and it is important to study the behaviour of the δ-ferrite at high temperature. The aim of this work is to investigate the influence of temperature and time of annealing on microstructure, especially the δ-ferrite behaviour.

Materials and Methods

The material used in this study is austenitic stainless steel that was delivered in hot rolled state. The chemical composition of steel is given in Table 1.

Table 1. *Chemical composition of tested austenitic stainless steel*

Chemical composition, wt./%							
C	Si	Mn	Cr	Ni	P	S	N
0.08	3.81	7.0	18.0	8.0	0.008	0.015	0.162

Specimens for testing were cut from the same bar with diameter of 15 mm. Before testing, all specimens were solution annealed at 1,020°C for 60 min followed by water quenching that brings precipitated carbides and most other intermetallic phases back into solution [4]. Later, the specimens were annealed at 750°C and 850°C for 5, 15, 30, 60, 120 and 180 min followed by cooling in the air. The microstructural analysis was carried out using the Olympus optical microscope and the scanning electron microscope (SEM) equipped with energy-dispersive spectrometer (EDS). Murakami's reagent (10 g $K_3Fe(CN)_6$, 10 g NaOH and 100 mL H_2O) was used for etching. Murakami's reagent at room temperature was used for identifica-

tion of carbides while heated reagent at 100°C was used for identification of the δ-ferrite and σ-phase. The δ-ferrite content and degree of its decomposition were determined by a Feritscope MP30 (Fisher, Germany). This is the magnetic induction method that takes advantage of fact that the δ-ferrite is magnetic while the austenite, carbides and σ-phase are not nonmagnetic microconstituents. The average value was calculated on the basis of five measurements (ASTM A800/A800M-91). Hardness test, according to standard BAS EN ISO 6507-1:2018, was performed on specimens prepared for microstructure analysis.

Results and Discussion

Microstructure Analysis

The microstructure analysis after solution annealing shows the presence of two-phase microstructure. The microstructure consists of the δ-ferrite in an austenite matrix. The δ-ferrite is elongated in the rolling direction (Figure 1). Etching with Murakami's reagent at high temperature (90°C–100°C) coloured the δ-ferrite in brown. Also, it can be seen that these stringers of the δ-ferrite are homogeneous.

The results of microstructure analysis of specimens heat treated at 750°C and 850°C for 5, 15, 30, 60, 120 and 180 min are shown in Figures 2 and 3.

Figures 2 and 3 show the austenitic microstructure with precipitation of secondary phases on the δ-ferrite and austenitic grain boundaries. These figures show the presence of the σ-phase because Murakami's reagent colours the σ-phase in blue on high temperature. Presence of the σ-phase is noticed only on the δ-ferrite. SEM analysis of the tested sample annealed at 750°C and 850°C confirmed the transformation of δ-ferrite (Figure 4). Analysis confirmed that with increasing temperature and time the form of the δ-ferrite is changed. The form of the δ-ferrite is not more homogeneous and disintegration of the δ-ferrite could be seen. The nucleation of the σ-phase predominantly occurred at austenite/δ-ferrite grain boundaries (Figure 4) because grain boundaries and interfaces are the high-energy regions.

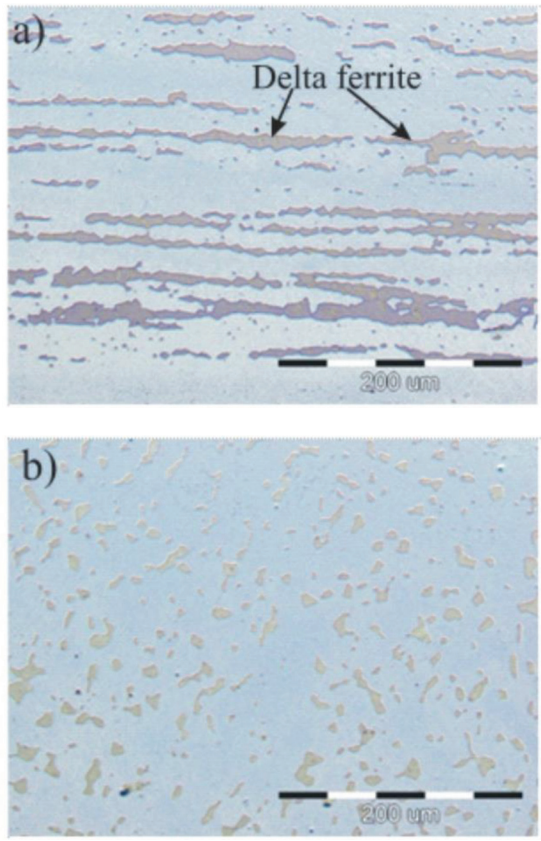

Figure 1. *Optical micrographs specimen in solution annealed state: (a) rolling direction and (b) transverse direction, Murakami's reagent (etching at high temperature), 200×.*

Table 2. *Energy-dispersive spectrometer analysis*

	Chemical composition, wt.%			
	Si	Cr	Fe	Ni
Spectrum 1	5.01	33.27	55.65	4.1
Spectrum 2	4.57	26.28	60.73	6.11
Spectrum 3	3.52	20.01	67.04	7.80
Spectrum 4	3.57	20.35	67.92	8.16

The average composition of the σ-phase was determined by EDS analysis and presented in Figure 5 and Table 2. The results show that the σ-phase mostly consists of Cr and Fe.

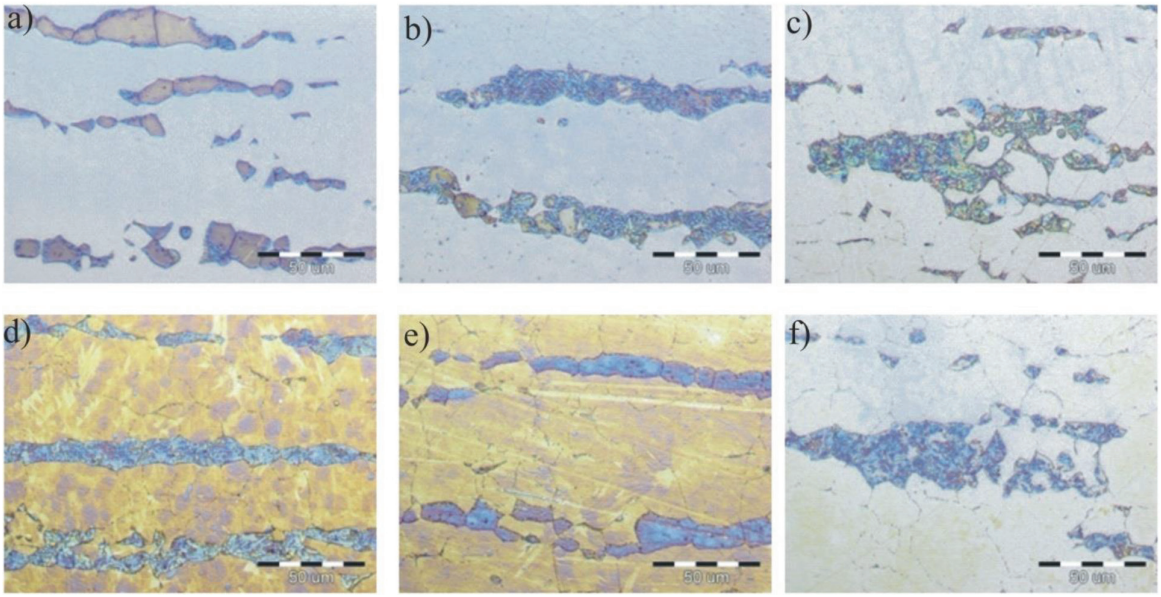

Figure 2. *Optical micrographs specimen heat treated at 750°C for (a) 5, (b) 15, (c) 30, (d) 60, (e) 120 and (f) 180 min, Murakami's reagent (etching at high temperature), 500×.*

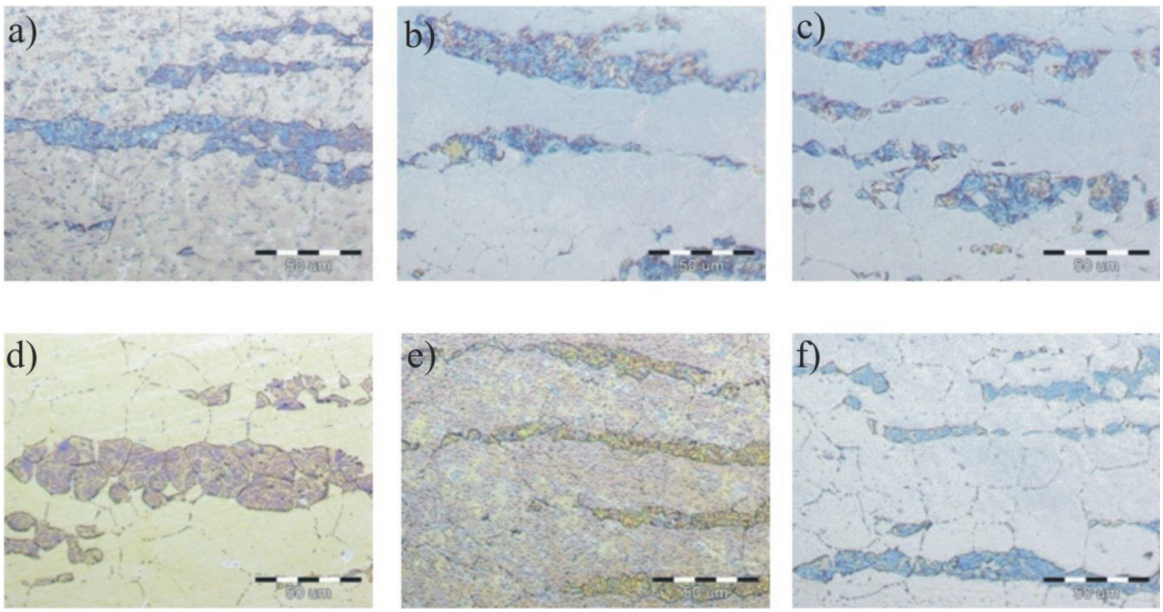

Figure 3. *Optical micrographs specimen heat treated at 850°C for (a) 5, (b) 15, (c) 30, (d) 60, (e) 120 and (f) 180 min, Murakami's reagent (etching at high temperature), 500×*

Although the literature considers the existence of other phases like carbides, analysis by SEM and EDS did not show their presence. To investigate the presence of carbides, etching with Murakami's reagent on room temperature was used. Etching at room temperature, carbides can be revealed at the austenite grain boundaries, within the weldment and the δ-ferrite [11]. Figure 6 show the presence of the carbides at austenite/δ-ferrite grain boundaries and in the δ-ferrite. At temperature 850°C, carbides were present at austenite grain boundaries too.

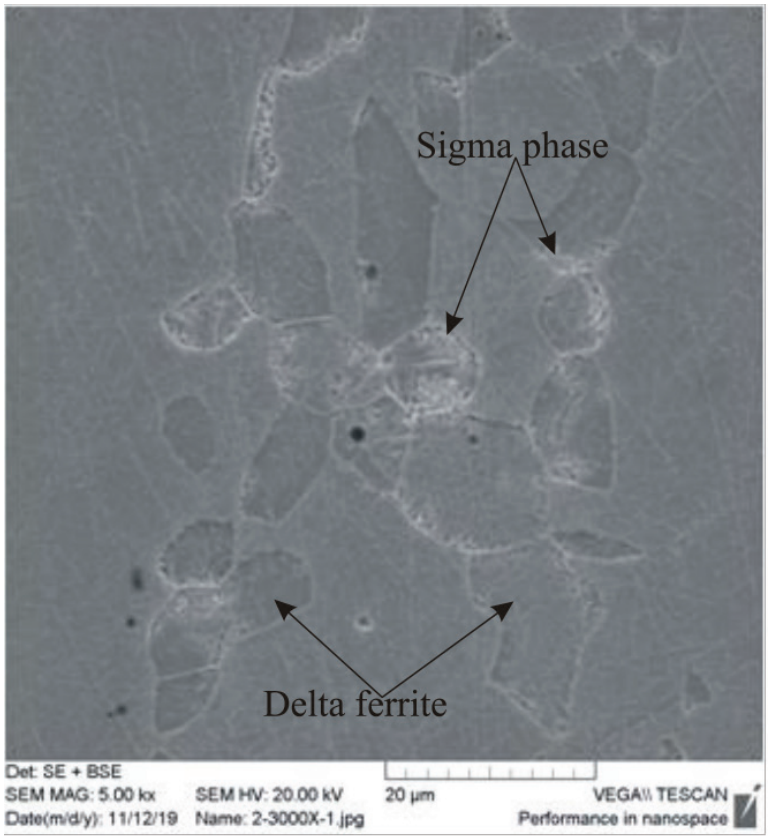

Figure 4. *Micrograph of transformation of the δ-ferrite using scanning electron microscope after annealing at 750°C for 5 min, 3,000×.*

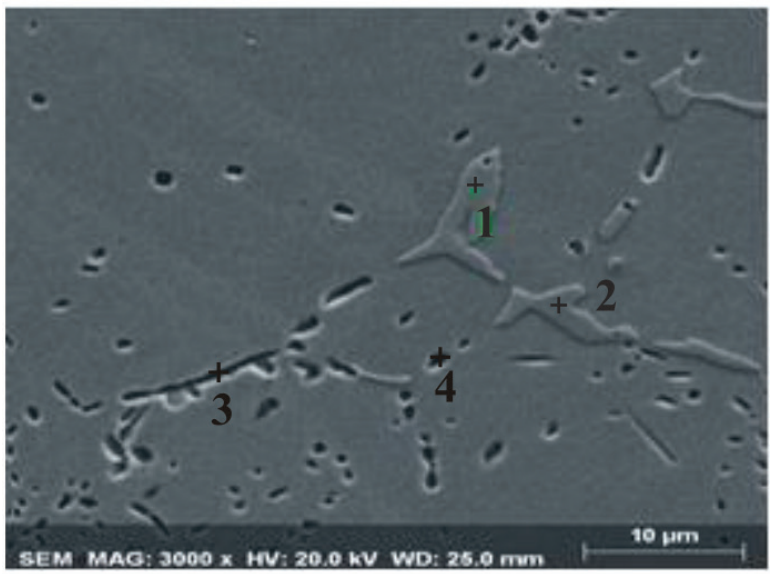

Figure 5. *Micrograph of σ-phase using scanning electron microscope after annealing at 750°C for 30 min, 3,000×.*

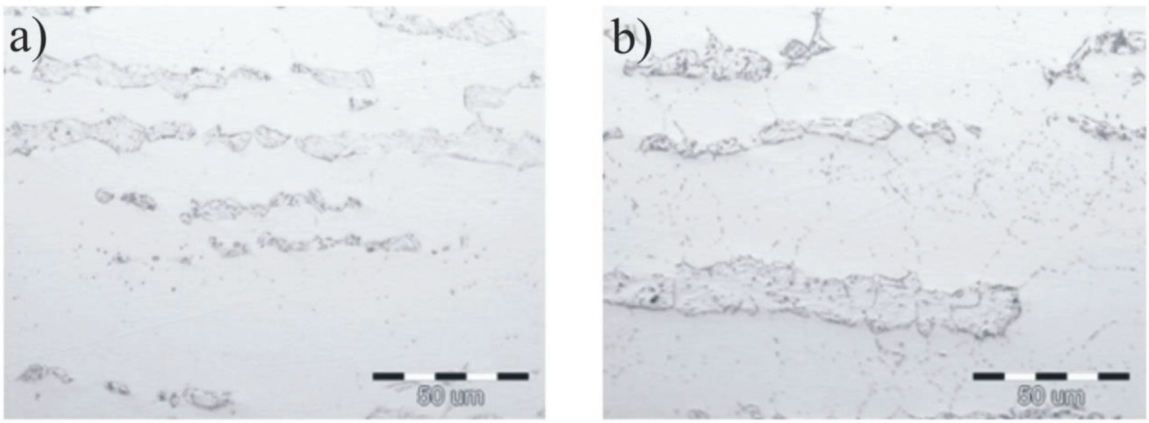

Figure 6. *Optical micrographs specimen heat treated: (a) at 750°C for 30 min (cooling in air) and (b) at 850°C for 30 min (cooling in air), Murakami's reagent (etching at room temperature), 500×.*

Determination of the δ-ferrite Content

Feritscope MP30 was used for the determination of the δ-ferrite content. Work of this device is based on the principle of magnetic induction, i.e. the δ-ferrite is magnetic and the austenite, σ-phase and carbides are nonmagnetic microconstituents. The results of testing are present in Figure 7. The average value of the δ-ferrite in initial solution annealed state was 12.42%.

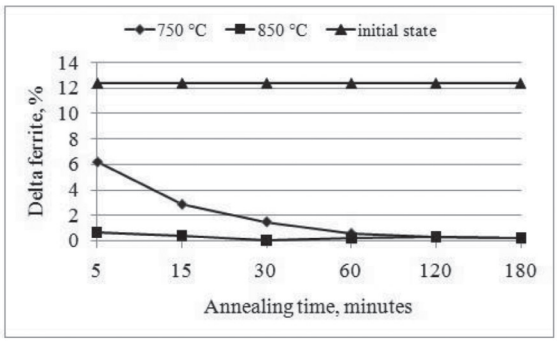

Figure 7. *The δ-ferrite content in annealed samples.*

Figure 7 shows that with increasing temperature or time the δ-ferrite content decreases compared with an initial state. The time of annealing has strong influence because after 1 h of annealing the δ-ferrite content is the same for both temperatures.

Hardness Testing

The hardness was tested on samples prepared for metallographic analysis according to standard BAS EN ISO 6507-1:2018. The samples were taken in the rolling direction. The results of the hardness testing are presented in Figure 8.

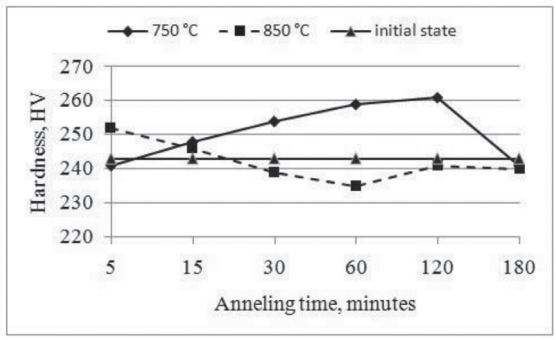

Figure 8. *Hardness testing for different temperatures and time.*

The testing of hardness showed that with increasing annealing time at 750°C hardness increases to 120 min, and later hardness decreases on the hardness of initial state. Hardness decreases with increasing annealing time at 850°C, but after 1 h hardness increases on the hardness of initial state. Influence of temperature on hardness was the opposite. After 5 min of annealing, the highest decomposition of the δ-ferrite was at 850°C (about 95%, almost two times more than at 750°C) and for those samples the hardness was the highest. However, the hardness decreases with increasing annealing time to 1 h. Then the hardness increases

to the initial state hardness. In case of annealing at 750°C, the situation is opposite, i.e. the hardness increases to 2 h of annealing than it decreases to the initial state hardness. After 3 h of annealing, the hardness is the same for both temperatures and it is almost the same as the initial state hardness.

Conclusions

From the results of investigation of influence of temperature and time on microstructure of austenitic stainless steel, i.e. decomposition of the δ-ferrite the following could be concluded:

- Initial microstructure of steel after solution annealing is austenitic with average value of 12.42% of the δ-ferrite.
- Increase in temperature and time of annealing resulted in decomposition of the δ-ferrite. After 30 min of annealing, content of the δ-ferrite was reduced to less than 2%, i.e. about 90% the δ-ferrite was transformed.
- Influence of temperature on decomposition of the δ-ferrite decreases with time because after 1 h annealing the ratio of decomposed δ-ferrite was the same for both temperatures. Temperature and time are very important for a diffusion process. It is possible to get the same results for higher temperature and shorter time or vice versa.
- Etching with Murakami's reagent on room temperature showed the presence of the carbides. Precipitation of the carbides was the first on austenite/δ-ferrite grain boundaries and in the δ-ferrite. With increasing temperature and time, the carbides were precipitated on austenitic grain boundaries too.
- After 180 min, hardness of annealed samples at 750°C and 850°C is almost the same as the initial state.

References

[1] Tehovnik, F., Vodopivec, F., Kosec, L., Godec, M. (2006): Hot ductility of austenite stainless steel with a solidification structure. *Materiali in tehnologije*, 40(4), pp. 129–138.

[2] Koseki, T., Inoue, H., Morimoto, H., Ohkita S. (1995): *Prediction of Solidification and Phase Transformation of Stainless Steel Weld Metal*s, Report No. 65, Nippon Steel Technical.

[3] Kožuh, S., Pavičić, K., Ivanić, I., Bizjak, M., Gojić, M. (2019): The effect of Annealing Time on Microstructure and Impact Energy of Stainless Steel AISI 316L. In: *Proceedings of 18th International Foundrymen Conference, Coexistence of material science and sustainable technology in economic growth*, Sisak, Croatia, Dolić, N., Zovko-Brodarac, Z., Begić-Hadžipašić, A. (eds.). University of Zagreb, Faculty of Metallurgy: Sisak, pp. 275–287.

[4] Barcik, J. (1988): Mechanism of σ-phase precipitation in Cr-Ni austenitic steels. *Materials Science and Technology*, 4(1), pp. 5–15, doi.org/10.1179/mst.1988.4.1.5.

[5] Folkhard, E. (1988): *Welding Metallurgy of Stainless Steels*. Springer-Verlag: Wien, 279 p.

[6] Yushchenko, K.A., Savchenko, V.S., Solokha, A.M., Voronin, S.A., (1993): Effect of Delta-Ferrite on the Properties of Welds in Austenitic Steels at Cryogenic Temperatures. *Advances in Cryogenic Engineering Materials*, 40(A), pp. 1263-1266.

[7] Astaf'ev, A.A., Lepekhina, L.I., Batieva N.M. (1989): Effect of delta-ferrite on the properties of welded joints of steel 08Kh18N10T. *Metal Science and Heat Treatment,* (31), pp. 880–884.

[8] Llorca-Isern, N., López-Luque, H., López-Jiménez, I., Biezma, M. V. (2016): Identification of sigma and chi phases in duplex stainless steels. *Materials Characterization,* (112), pp. 20–29, doi.org/10.1016/j.matchar.2015.12.004.

[9] Padilha, A.F., Rios, P.R. (2002): Decomposition of Austenite in Austenitic Stainless Steels. *ISIJ International*, 42(4), pp. 325–337, https://doi.org/10.2355/isijinternational.42.325.

[10] Khatak, H.S., Raj, B. (2002*): Corrosion of Austenitic Stainless Steels: Mechanism, Mitigation and Monitoring*. Narosa Publishing House: New Delhi, 385 p.

[11] Identification of Phases in Stainless Steels by Etching. G.V. Voort, [cited 30/01/2019], Available on: *https://vacaero.com/information-resources/metallography-with-george-vander-voort/1061-identification-of-phases-in-stainless-steels-by-etching.html.*

Original scientific paper

Received: Apr 29, 2020
Accepted: May 18, 2020
DOI: 10.2478/rmzmag-2020-0008

Key Metallurgical Parameters of Fe-Ni Production During 1984–1997 and 2007–2017 at the Ferronickel Smelter in Drenas

Ključni metalurški parametri proizvodnje Fe-Ni med letoma 1984 in 1997 ter 2007 in 2017 v topilnici feroniklja v Drenasu

Zarife Bajraktari-Gashi[1,*], Muharrem Zabeli[1], Behram Halilaj[2]

[1] Faculty of Geoscience, Department of Materials and Metallurgy, University of Mitrovica "Isa Boletini", St. Ukshin Kovacica, 40000, Mitrovica, Kosovo

[2] New Foundry of the New Ferronickel in Drenas, Kosovo

* zarife.bajraktari-gashi@umib.net

Abstract

During 1984–1997, the ferronickel plant in Drenas used iron-nickel ore from the mines of the Republic of Kosovo: Glavica and Çikatove (Dushkaje and Suke) mines. However, during the years 2007–2017, when the plant started operating from the cessation of production, which was from 1998 to 2007, some types of iron-nickel ores from different countries began to be used, starting from iron-nickel ores from Kosovo, iron-nickel ores from Albania, ores from Indonesia, ores from the Philippines, ores from Guatemala, ores from Turkey and ores from Macedonia. The ore composition, however, is mainly oxide-laterite ore. Iron-nickel ores in the plant are characterised by high moisture content, a very important factor influencing the process of scraping the charge in rotary kilns and presenting in general. Among the iron-nickel ore used in the ferronickel plant, the ores from Albania are characterised due to their low moisture content when compared with the other ores as well as the high content of iron oxides, which affect the temperature rise inside the furnaces, as the iron ores play an important role in the pre-casting process in rotary kilns.

Key words: calcine, alloys, ore, foundry, Fe-Ni alloy.

Povzetek

Med letoma 1984 in 1997 je topilnica feroniklja v Drenasu uporabljala železo-nikljevo rudo iz rudnikov v Kosovem: rudniki Glavica in Cikatove (Dushkaje in Suke). Med letoma 2007 in 2017, potem ko je po zaprtju v obdobju od 1998 do 2007 proizvodnja ponovno začela obratovati, pa so začeli uporabljati železo-nikljevo rudo iz drugih držav, kot so: železo-nikljeve rude iz Kosova, železo-nikljeve rude iz Albanije, rude iz Filipinov, rude iz Guatemale, rude iz Turčije in rude iz Makedonije. Sestava omenjenih rud temelji na oksidno-lateritni osnovi. Za železo-nikljeve rude je značilna visoka vsebnost vlage, kar je zelo pomemben dejavnik pri procesu plavljenja rude, ki vpliva na splošen potek plavljenja in postopek strganja vložka v rotacijskih pečeh. Med železo-nikljevimi rudami, ki se uporabljajo v topilnici feroniklja, je za rudne iz Albanije značilna nizka vsebnost vlage in velik delež železovih oksidov v primerjavi z drugimi rudami. Velik delež oksidov vpliva na povišanje temperature v rotacijskih pečeh, kjer železove rude igrajo pomembno vlogo tudi pri procesih, ki se vrstijo pred litjem.

Ključne besede: žganje, zlitine, rude, talilnica, Fe-Ni zlitina.

Introduction

The new Foundry of the new Ferronikel in Drenas is located near the source "Old Çikatove" 37 km northwest of Prishtina. The production of metallurgy until now in the Republic of Kosovo is oriented in processing ore of local mines, such as Golesh and Çikatove, and imported ore (from the year 2007) from Indonesia, Philippines, Guatemala, Albania, Macedonia and Turkey.

The processing is done using the electro-reduction process to prepare Fe-Ni as the final product. The fundamental establishments and the equipment of the foundry are two rotary kilns of the firm "Schmid" Copenhagen, two rotary kilns of the firm "Elkem"-Spikerverket, Oslo and two convertors LD of the firm Krupp, Dusseldorf [1].

In the new foundry in the new Ferronickel in Drenas, the process of Fe-Ni production passes through the following stages: processing of Fe-Ni ore and fuels and their delivery to appropriate bunkers where with the aid of conveyor belts they enter the rotary kiln. At a temperature of over 500°C using special equipment, the fuel enters, consisting of heavy-oil and pet - kok, that influence the temperature increase of the rotary kiln (over 700°C) and the qualitative production of calcine [2]. The calcine produced by the rotary kilns is sent to the electric furnace through special pipes where the Fe-Ni metal production process and the quantity of slag are realised.

The produced metal from the electric furnace is sent to the converter for refining, in which an amount of limestone is introduced, and oxygen is blown into it. After the refining, metal is poured into special equipment where we have the production of Fe-Ni metal, in the form of granules of the size of 15–20 mm and weight 5–15 g while the remaining slag in the converter is divided into the metallic part and the non-metallic part, where the metallic part gets back in the process [3].

In the new foundry of the new Ferronickel in Drenas during the realisation in 2007–2017, these Fe-Ni ores were used: ores from Kosovo (mines: Gllavice and Qikatove), ores from Albania, ores from Guatemala, ores from Indonesia, ores from the Philippines, ores from Turkey and ores from Macedonia. The composition of the ores is oxide and silicate. The annual average of Ni content in the Guatemala, Philippines, Indonesia ore is higher (Ni = 2%) compared with the Kosovar ore (Ni = 1.5%) and Albanian ore (0.99%) [3].

Working methods

The industrial data are parameters based on the production process of ferronickel in Drenas, during the years 1987–1997, and the industrial production period of Fe-Ni during the years 2007–2017, directly from the production process of the Fe-Ni alloy [1, 3].

During the industrial processes of the analyzed years, we have determined:

- The average of Fe-Ni ore in rotary kilns,
- The average amount of calcine produced from both rotary kilns (Figure 1),
- Amount of Fe-Ni from the electric furnace,
- The average of Ni in tons.

Discussion of results

The research during the years 1984–1997 is based on the data from the archive of the ferronickel Plant, whereas the research during the years 2007–2017 is based on the laboratory and industrial work of the Fe-Ni alloy production in the Plant.

Figure 1 represents the production data of the iron-nickel, starting from:

- Average of Fe-Ni ore,
- Calcine average,
- Average of Fe-Ni alloy,
- Obtained average of Ni in tons [1–4].

The obtained amount of calcine during the years 2007–2017 is 40% higher than the calcine amount obtained during the years 1984–1997, a difference which comes as a result of a few factors.

During the years 1984–1997, the Plant's start is accompanied with great difficulties, among them the inability of reaching the high temperatures of 900–1000°C as provided by the Gipronickel project (the Plant project of 1983), which was a big problem because the tempera-

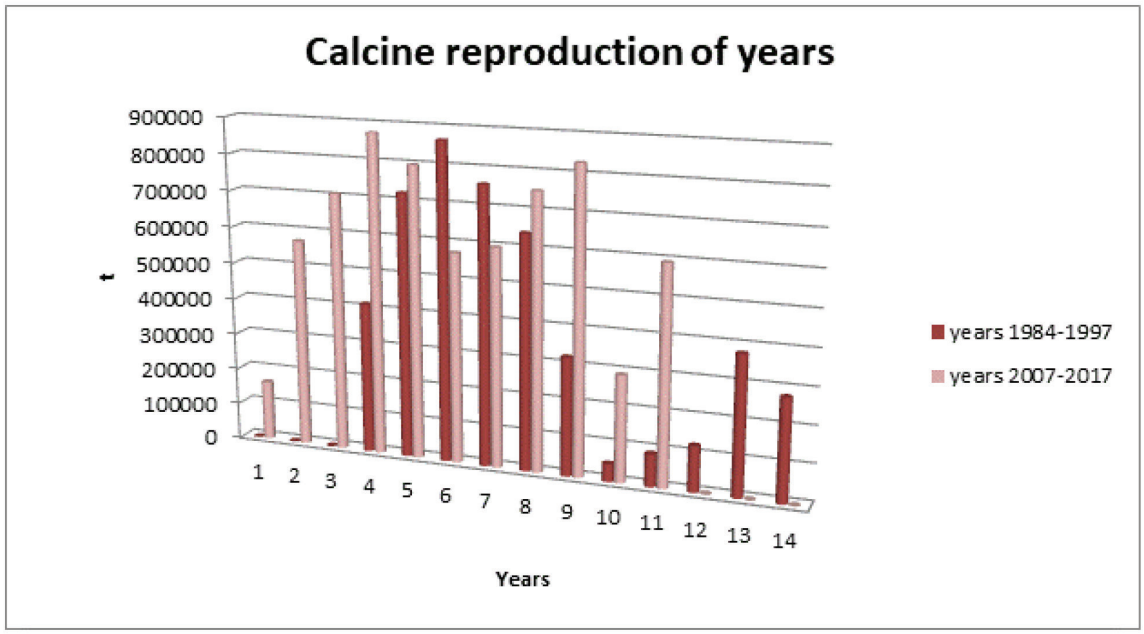

Figure 1: *The produced calcine during the analyzed years.*

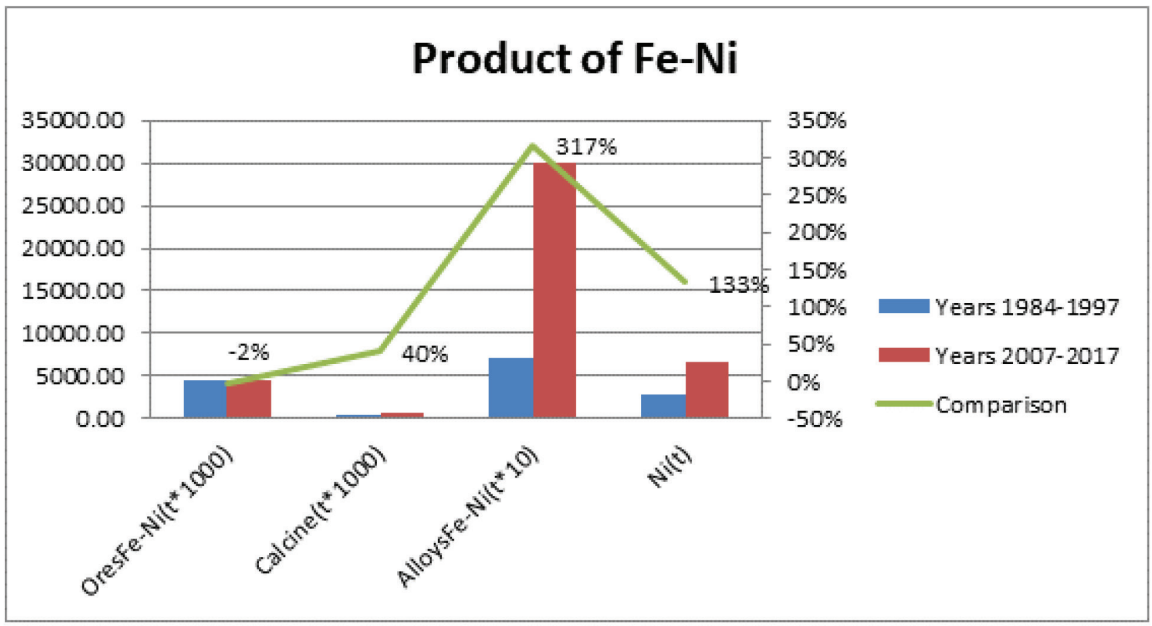

Figure 2: *Graphical representation of Fe-Ni products: the amount of Fe-Ni ore, calcine, Ni in tons and the Fe-Ni alloy as a final product of the process.*

ture plays a crucial role in the process of rotary kilns and the development of pyrometallurgical processes in general [1].

The amount of calcine produced during the years 1984–1997, followed by very high impurity, was frequently interfered within the manufacturing process for the possibility of achieving production parameters as provided by the project (according to the archive and engineering of that time). These were the factors that influenced the low production of both Fe-Ni and Ni quantities in tons, compared with higher production quantities during 2007–2017. During the years 2007–2017, some changes

(a) (b)

Figure 3: *The two forms of Fe-Ni alloy production. (a) The shape of big blocks; (b) The shape of granules.*

were made to the ferronickel plant in Drenas which resulted in the higher production of Fe-Ni alloy:

- Placement of Fe-Ni ore dryer during the years 2010–2012 [4].
- The Albanian ores influenced the reduction of limestone. During the years 1984–1997, the used amount of limestone in the charge was 5%, whereas during the years 2007–2017, it dropped to 2% $CaCO_3$.
- The converter slag and calcine parts returned to the rotary kiln process during 2010 and onwards [5].
- Starting from 2013, there is a change in the production of the physical form of the Fe-Ni alloy.
- Until 2013, the Fe-Ni alloy had the form of big blocks weighing 25 kg, as shown in Figure 3, whereas starting from 2013, the physical form of the Fe-Ni alloy has the shape of a granule around 15–20 mm. The reason behind the change in physical form was the greater possibility of melting for the usage in special steel production [1].

Conclusions

From the analysis of research done during the years 1984–1997 and 2007–2017, we can conclude that as a result of the changes made during the years 2007–2017, we have a higher amount of iron-nickel alloy production [1, 2].

During the laboratory and industrial research of the production parameters analysis 1984–1997 (based on the plant archive) and the years 2007–2017, we may conclude that we analyzed the first 13 years when the ferronickel plant started operating for the first time and the 10 years when the plant started operating again [1, 4].

From the research made, it is clear that the amount of ore input in rotary kilns does not change much, varying only by a 2% increase during the period of 1984–1997; however, the amount of calcine obtained by rotary kilns is 40% higher during the years of 2007–2017, even though the higher ore input of 1984–1997 should have correlated with a higher calcine output [1, 5].

During the research, we have concluded that the low calcine output of the years 1984–1997 is a result of the high impurities which followed the ore and calcine obtained and the frequent cessation of the rotary kilns due to their inability of reaching the adequate temperatures.

From the research we obtain the main parameter of the production of the plant, Fe-Ni alloy is very high during 2007–2017. Changes made during 2007 and 2017 were the major factors in the greater benefits of Fe-Ni alloy production parameters [3].

Recommendations

1. Placement of dryer for iron-nickel ore.
2. The ore with the highest moisture content should be placed inside the dryer.
3. The amount of ore during autumn and winter should be covered in the premises of the Plant.

Acknowledgements

Funding

No funding has been given to support this research.

Conflicts of Interests

Authors declare that they have no known competing financial interests or personal relation-

ships that could have appeared to influence the work reported in this paper.

Availability of data and material

The research has been conducted thanks to the data of the Ferronickel archive, concerning the data needed from 1984 to 1997, whereas the rest of the research including the parameters for the years 2007–2017, has been conducted at the Ferronikel Foundry in collaboration with Behram Halilaj.

Author's contributions

This research paper has been realised by my work as the main author, as well as the contribution of Muharrem Zabeli and Behram Halilaj as corresponding authors.

References

[1] Official Documentation of Melting Complex of New Ferronickel Complex L.L.C. Gllogoc, 1984–1997 and 2009–2017.

[2] Bajraktari Gashi, Z., Zabeli, M., Halilaj, B. (2018): The impact of Pet-Kok in The Technological Process of Production of Fe-Ni in the New Foundry of the New Ferronickel in Drenas. *Journal of International Environmental Application and Science*, 13, pp. 72–77.

[3] Bajraktari Gashi, Z., Halilaj, B. (2018): Material Balance of the Technological Process in the New Foundry of New Ferronikel in Drenas During 2017. *Journal of Technology and Exploitation in Mechanical Engineering*, 4, pp. 29–35.

[4] Bajraktari Gashi, Z. (2012): *Theoretical and Experimental Research in Order to Reach Optimum Technical, Technologic and Productive Parameters During Qualitative Reduction of Ni ore in Fe-Ni foundry in Drenas*. Ph.D. Thesis. University of Prishtina 'Hasan Prishtina', Faculty of Geoscience and Technology, Department of Materials and Metallurgy: Prishtina, 108 p.

[5] Bajraktari Gashi, Z., Imeri, Sh., Lohja, N., Zabeli, M., Tahiraj, N., Murati, N. (2011): Experimental Research on Pre-Reduction of Nickel Silicate Ore in New Ferronickel Factory in Drenas. *WSEAS and NAUN Conferences*, pp. 306–311.

[6] Bajraktari Gashi, Z., Maksuti, Rr., Murati, N. (2015): The Usage of Pet Kok is a Possibility of Reducing the Amount of Heavy Oil in the Rotary Kilns in the New Foundry of the New Ferronikel in Drenas. *Applied Mechanics and Materials*, 749, pp. 111–115, DOI: 10.4028/www.scientific.net/AMM.749.11.

Original scientific paper

Received: Apr 30, 2020
Accepted: May 18, 2020
DOI: 10.2478/rmzmag-2020-0006

Petrography of Allanite-bearing Tonalite from Iwo Region, Osun State, Nigeria

Petrografija tonalita z alanitom iz območja Iwo, Osun State, NIgerija

Oziegbe E.J.[1,*], Ocan O.O.[2], Buraimoh A.O.[1]

[1] Department of Geosciences, Faculty of Science, University of Lagos, Nigeria

[2] Department of Geological Science, College of Science, Engineering and Technology, Osun State University, Nigeria

* eoziegbe@unilag.edu.ng

Abstract

Primary, secondary and accessory minerals in tonalitic rocks from Iwo region of the Precambrian Basement Complex of Southwestern Nigeria were identified and analysed with the aim of determining the various processes involved during the crystallisation of magma. Thin sections of tonalite were prepared and studied with the aid of a petrographic microscope. The mineral assemblages observed are biotite, plagioclase, alkali-feldspar, amphiboles, pyroxene, quartz, muscovite and chlorite. Allanite, titanite, apatite and zircon occur as accessory minerals. Muscovite and chlorite are found to be secondary minerals. The mineral allanite has a characteristic form of zoning and shows evidence of metamictisation, and is surrounded by dark-coloured biotite having radioactive haloes. Titanite is anhedral to subhedral crystals and forms reaction rim round opaque minerals. Plagioclase shows evidence of compositional zoning as well as plastic deformation of the twin lamellae. The allanite observed is primary in nature and has undergone radioactive disintegration; chlorite and muscovite are formed by secondary processes of chloritization and sericitisation, respectively. The tonalite is formed as a result of rapid cooling of magma close to the Earth's surface.

Keywords: zoning, titanite, radioactive haloes, chloritization, sericitisation.

Povzetek

Z namenom določevanja različnih procesov, ki so vključeni pri kristalizaciji magme, so bili identificirani in opisani primarni, sekundarni in akcesorni minerali v tonalitnih kamninah iz pred-kambrijske podlage območja Iwo v jugozahodni Nigeriji. Zbruski tonalita so bili pripravljeni in raziskovani s pomočjo petrografskega mikroskopa. Opazovani minerali so: biotit, plagioklaz, alkalijski glinenec, amfibol, piroksen, kremen, muskovit in klorit. Alanit, titanit, apatit in cirkon se pojavljajo kot akcesorni minerali. Ugotovljeno je, da se muskovit in klorit pojavljata kot sekundarna minerala. Mineral alanit ima karakteristično obliko conarnosti in kaže prisotnost metamiktizacije ter je obkrožen s temno obarvanim biotitom z radioaktivnimi haloi. Titaniti so anhedralni do subhedralni kristali in tvorijo reakcijski obroč okrog neprozornih mineralov. Plagioklaz kaže prisotnost kompozicijske conarnosti in plastične deformacije dvojčičnih lamel. Alanit je naravno primaren in je prestal radioaktiven razpad, klorit in muskovit sta nastala kot sekundarna procesa kloritizacije in sericitizacije. Tonalit je nastal kot rezultat hitrega ohlajanja magme v bližini zemeljskega površja.

Ključne besede: conarnost, titanit, radioaktivni halo, kloritizacija, sericitizacija.

Introduction

Iwo region, the area under study, is part of the Precambrian of Southwestern Nigeria, which is part of the Nigerian Basement Complex (Figure 1). Iwo region comprises of a migmatite-gneiss-granite complex and a metasupracrustal sequence (Figure 2). In addition to a widespread metasomatism that is a feature of this region, there is also the occurrence of early tonalitic and syenitic diapirs and late magmatic, granitic, pegmatitic, and aplitic intrusions in the large Iwo-Ikire complex [1]. Tonalite that is present in the study area belongs to the Older Granite Complex that comprises rocks with varying composition from the granodiorite to true granite [2]. This range comprises rocks of varying compositions (granites, granodiorites, adamellite, quartz monzonites, syenites and pegmatites). In some cases, older granites have been reported to be foliated, defined by the alignment of the both feldspar crystals and mafic minerals [2]. Foliated older granites have been found in places such as Iwo, Idanre and Igarra in Southwestern Nigeria. However, it must be noted that older granites that have disordered arrangement of its feldspars are usually non-foliated. Rocks of Iwo area have been found to be affected by late reworking, metasomatism and granitic activity to varying extents [1]. Allanite ($CaREE(Al,Fe^{3+})\ 2(Mg,Fe^{2+})\ Si_3O_{12}(OH)$) is a common accessory mineral in granitic and rhyolitic rocks. Allanite is a major residence site for LREE [3, 4]. In some rocks, as

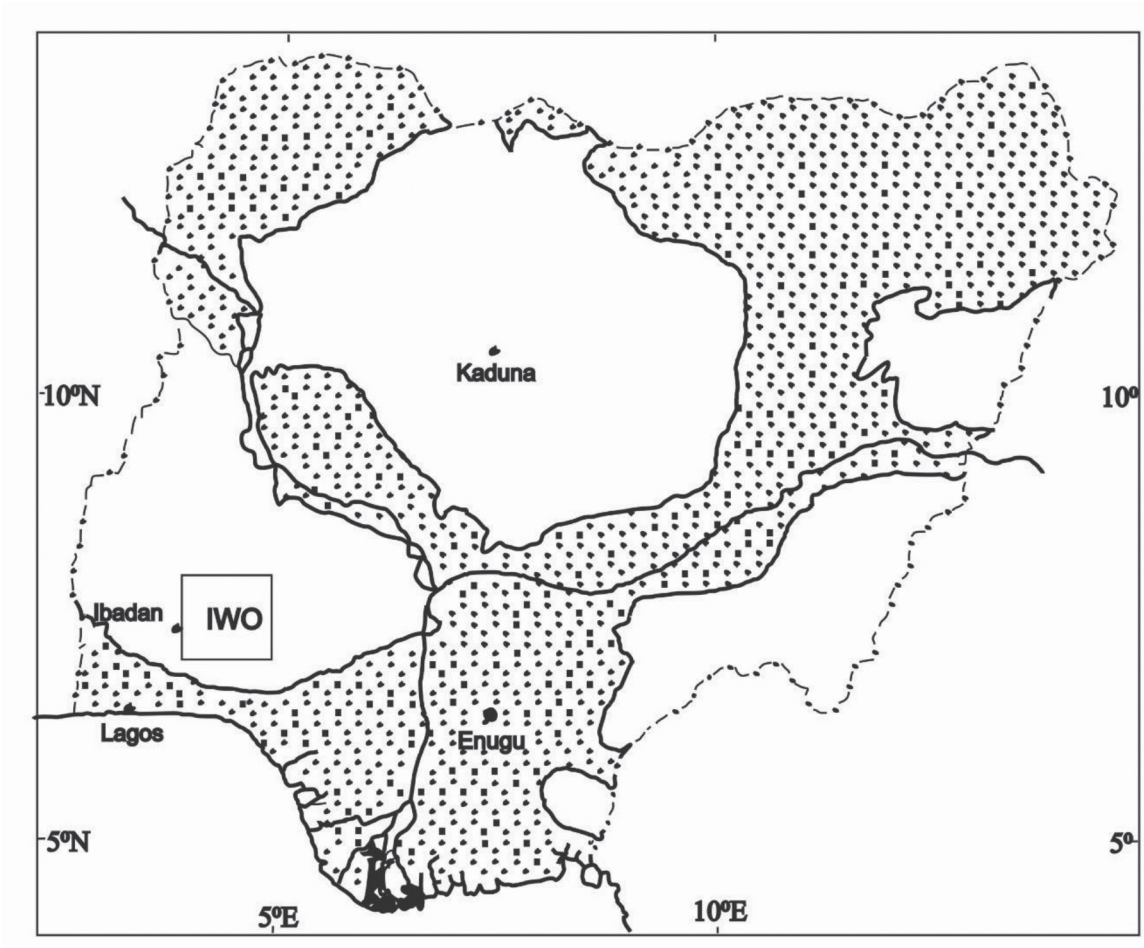

Figure 1: *Map of Iwo region within Basement Complex of Nigeria. Stippled pattern indicates Cretaceous and younger sedimentary cover [1].*

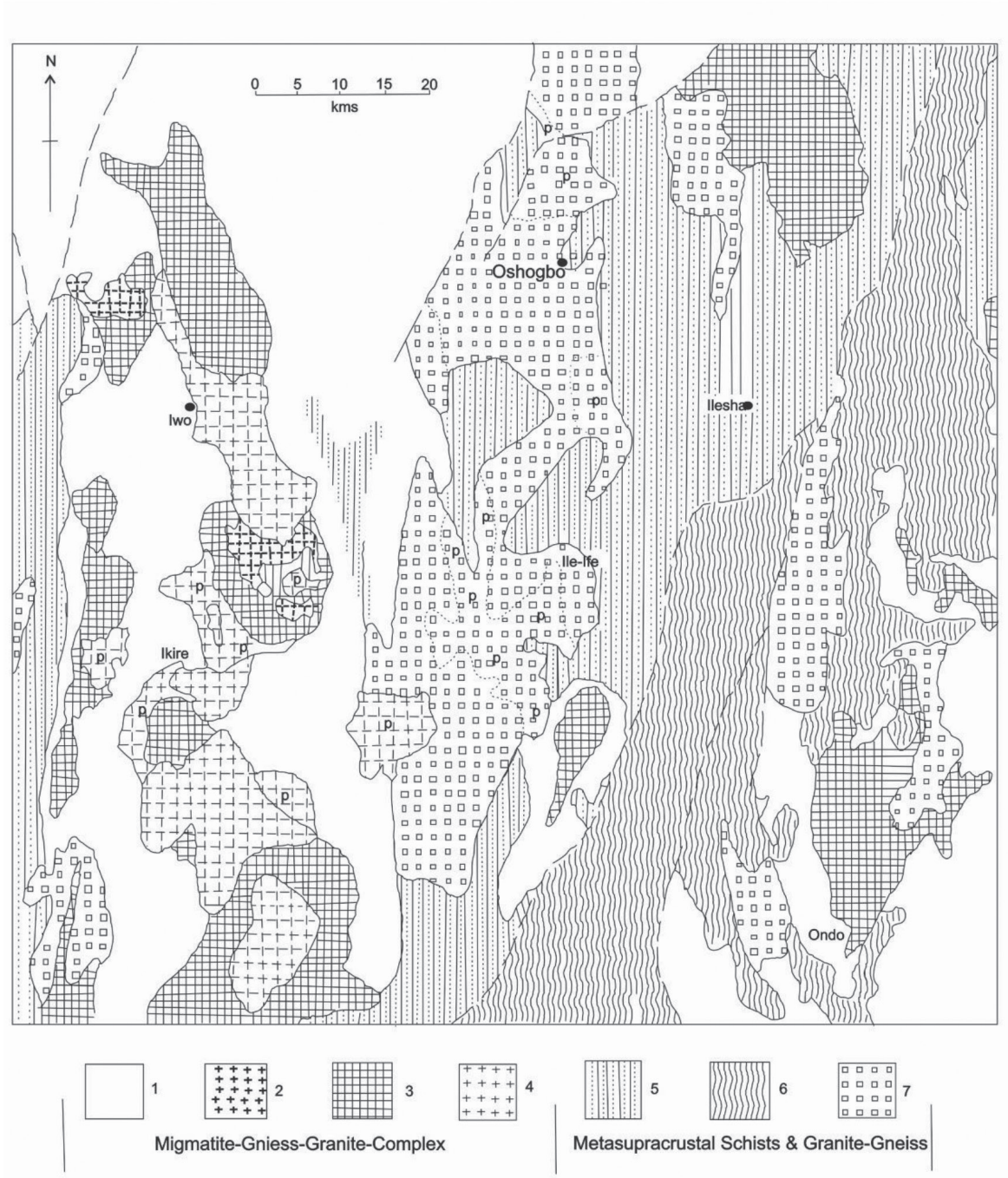

Figure 2: *Geologic map of Iwo region modified after 1: 250,000 sheet 60 (Iwo) of Geological Survey of Nigeria (GSN). 1, Migmatite-gneiss complex; 2, charnockite; 3, early granitic phases of Older Granite Cycle; 4, younger granitic phases of Older Granite Cycle; 5, amphibolite, amphibolite schist, and pelitic schist; 6 quartzite, quartz-schist, and quartzofeldspathic gneiss; 7, granitic-gneiss-dominated regions; p, pegmatite; T, tonalite. Thick broken lines indicate major faults [1].*

high as 50–80% of Ce and La have been found in allanite. As a result of this, allanite has been used to track the behaviour of REE during melting, crystallisation and other igneous processes [5–7]. Titanite is found in different geological environments. Both allanite and titanite are common accessory minerals found in hydrothermal deposits [8, 9].

The tonalite under study is coarse-grained and foliated (Figures 3 and 4); foliation is marked by preferred orientation of long axes of tabular microcline grains and the long axes of the maf-

Figure 3: *Field photograph showing tonalite. Take note of the vein quartz at the centre.*

Figure 4: *Hand specimen of tonalite from Iwo area.*

ic minerals (biotite and pyroxene). The objective of this work is to petrographically describe the mineral assemblages with emphasis on the accessory minerals, allanite and titanite. Rock samples were taken from the following localities in Iwo region: Adana, Elemo, Elewonta and Isero/Ikonifin.

Materials and Methods

Four rock samples were taken from four different locations. Sixteen thin sections of these rocks were prepared at the laboratory of the Department of Geology, Obafemi Awolowo University. Detailed study of the thin sections were done using petrographic microscope at the Department of Geosciences, University of Lagos. Photomicrographs of areas of interest were taken both under plane polarised light (PPL) and cross polarised light (XPL).

Results

Petrography

The rock is porphyritic in texture, with phenocrysts of K-feldspar and plagioclase in matrix of biotite, amphibole and quartz. The main minerals are microcline, biotite, plagioclase, whereas green non-pleochloric pyroxene, amphibole (green hornblende) and quartz occur as minor minerals. Chlorite and muscovite occur as secondary minerals. Accessory minerals are allanite, zircon, titanite (sphene), apatite and opaque minerals. Allanite crystals are zoned, reddish brown in colour and strongly pleochroic with euhedral and subhedral crystals (Figures 5–7). Some crystals of allanite are altered whereas others are not; those that are altered have inclusions of opaque minerals mostly concentrated at the core (Figure 5c). Biotite is brownish in colour and subhedral in form, intergrown with allanite (Figure 5a).

Biotite consists of other minerals such as apatite (Figure 6a). Crystals of biotite show altered surfaces and display a form of preferred alignment. There is a close association between biotite and chlorite which is in turn surrounded by titanite (Figures 8a and 8b), all of which are in the proximity of microcline (Figure 8b). The plagioclase feldspar shows sign of (i) compositional zoning and (ii) deformation (Figures 8c and 8d). Plagioclase exhibits a combination of albite and Carlsbad twinning. Crystals of biotite occur as inclusions in plagioclase. A few crystals of titanite are euhedral, but majority are subhedral/anhedral. The subhedral grains occur as aggregates and are clustered around biotite, chlorite and opaque minerals. The anhedral form of titanite forms reaction rim around opaque minerals (Figures 9–11). Titanite is concentrated in and around biotite (Figures 8a, 9 and 10). There is a close association between titanite and biotite, amphiboles, plagioclase, chlorite and opaque minerals. In some samples, the titanite crystals that form reaction rim round opaque minerals are in contact with biotite, amphibole and plagioclase (Figures 10 and 11).

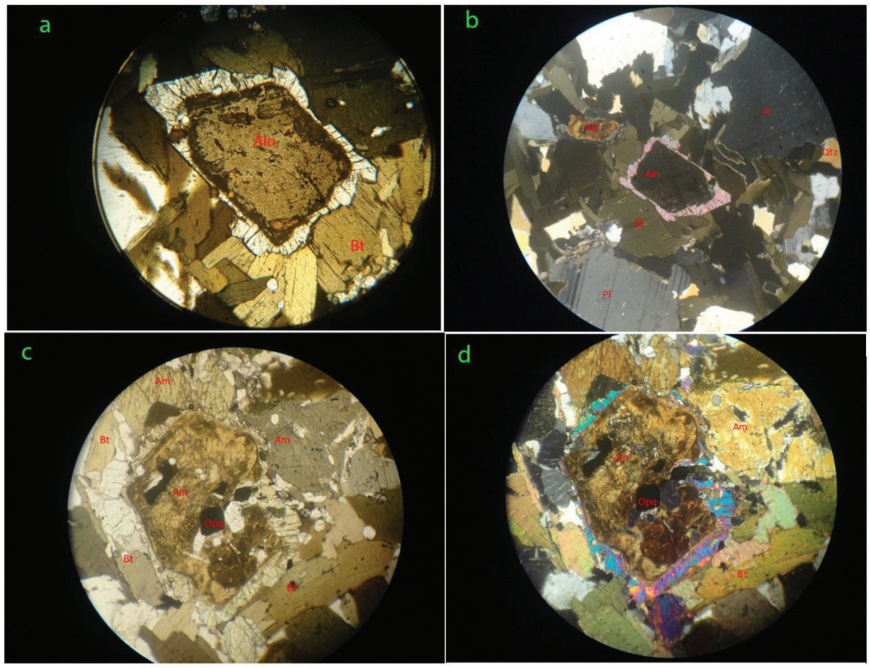

Figure 5: *Photomicrographs showing: (a) zoned allanite (Aln) surrounded by biotite (Bt) crystals; biotite is darker at the edges closer to allanite than those away (PPL). (b) Zoned allanite (Aln), biotite (Bt), plagioclase (Pl) and quartz (Qtz) (XPL). (c) Opaque (Opq) minerals within a zoned allanite (Aln), take note of the close relationship between biotite and allanite (PPL). (d) Inclusions of opaque (Opq) minerals within a zoned allanite (Aln) (XPL).*

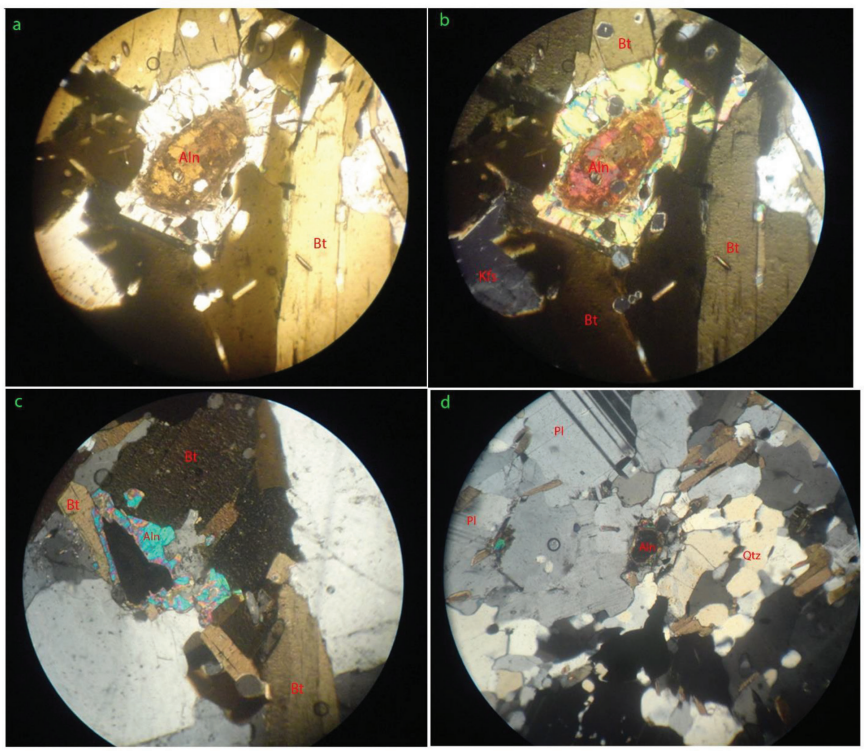

Figure 6: *Photomicrographs showing: (a) numerous fractures within zoned allanite (Aln), there are inclusions of apatite in biotite (Bt) and the edges of biotite touching allanite are darker (PPL). (b) Opaque (Opq) minerals within allanite (Aln) (XPL). (c) Biotite (Bt) surrounding allanite (Aln), there are inclusions of allanite within biotite (XPL). (d) Close association between plagioclase (Pl) and allanite (Aln) (XPL).*

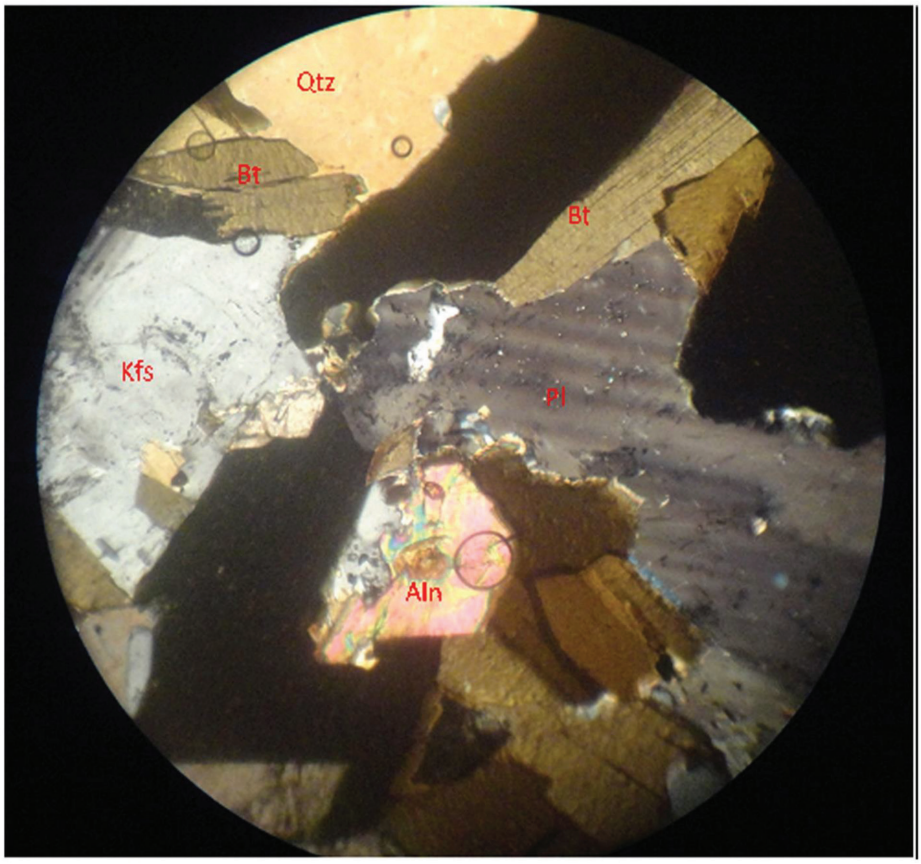

Figure 7: *Photomicrograph showing sericitisation of plagioclase feldspars (Pl) in close association with allanite (Aln) (XPL).*

Discussion

The early formed minerals observed in the tonalite are allanite, amphiboles, plagioclase and quartz. The presence of allanite within biotite and hornblende can be attributed to early crystallisation. Amphibole (hornblende) is not present in all of the samples studied. Primary allanite has inclusions of ilmenite and is included in biotite as observed in the rock samples [10]. Primary allanite has been found in andesitic [11] and tonalitic [12] igneous rocks. Allanite is a high-Th-REE mineral of the epidote group and has been used in recent times in Th–U–Pb geochronology [9, 13–18].

The accessory mineral allanite is highly prone to alteration as a result of its metamict ability and there are inclusions of opaque minerals within the altered region of the crystals (Figure 5c). The biotite crystals surrounding allanite have radiation haloes that are darker at the contact edges closer to allanite (Figures 5a and 6a). This complex radioactive rim is an evidence of post-crystallisation process [19]. Allanite is one of the most common sources of primary uranium-bearing minerals [19]. In addition to the radioactive rim, there are numerous fractures on the altered allanite (Figure 6a) which can be attributed to the radioactive process. The degree of metamictisation of allanite depends on the degree of alpha-recoil damage [20]. This metamictisation coupled with hydrothermal alteration results in a variety of alteration products that tend to immobilise the REE and Th^{4+} in more stable secondary phases [21]. These formed phases has been found to be dependent on the physiochemical condition of the fluid which is present. Allanite and titanite have the potential of controlling REE in granitic magmas [5]. Titanite observed are of both primary and secondary types: the primary types are subhedral to eudedral in shape with some occurring as inclusions in biotite and amphiboles. The titanite-opaque mineral phase observed is an indication of the breaking down of titanite

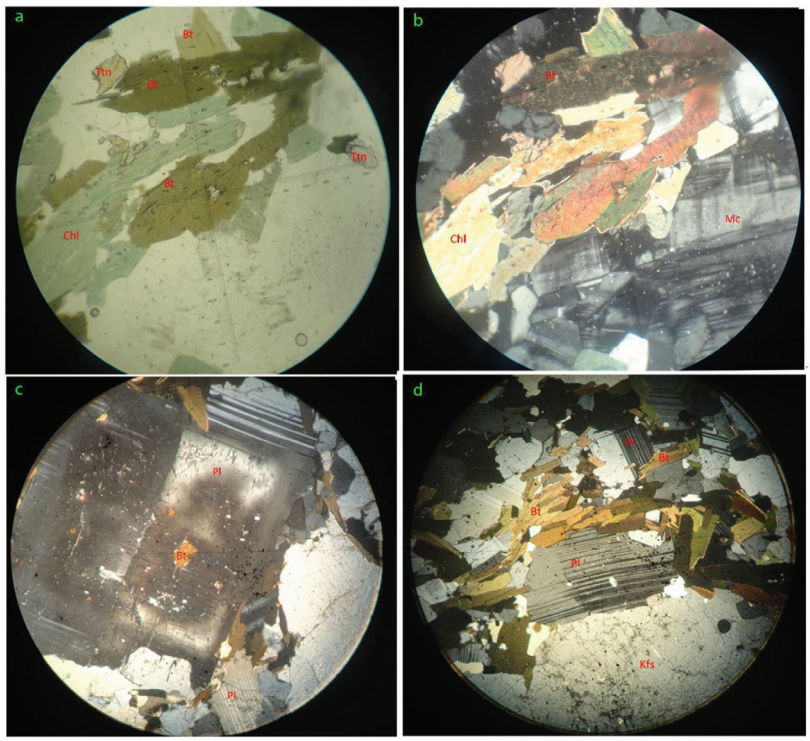

Figure 8: *Photomicrographs showing: (a) close association between biotite (Bt) and chlorite (Chl), as well as titanite (Ttn) (PPL). (b) Microcline (Mc) in close relationship with altered biotite (XPL). (c) Compositional zoning of plagioclase, there are biotite (Bt) inclusion in the plagioclase feldspar (Pl) (XPL). (d) Plagioclase with deformed twin lamellae and preferred orientation of the biotite (Bt) (XPL).*

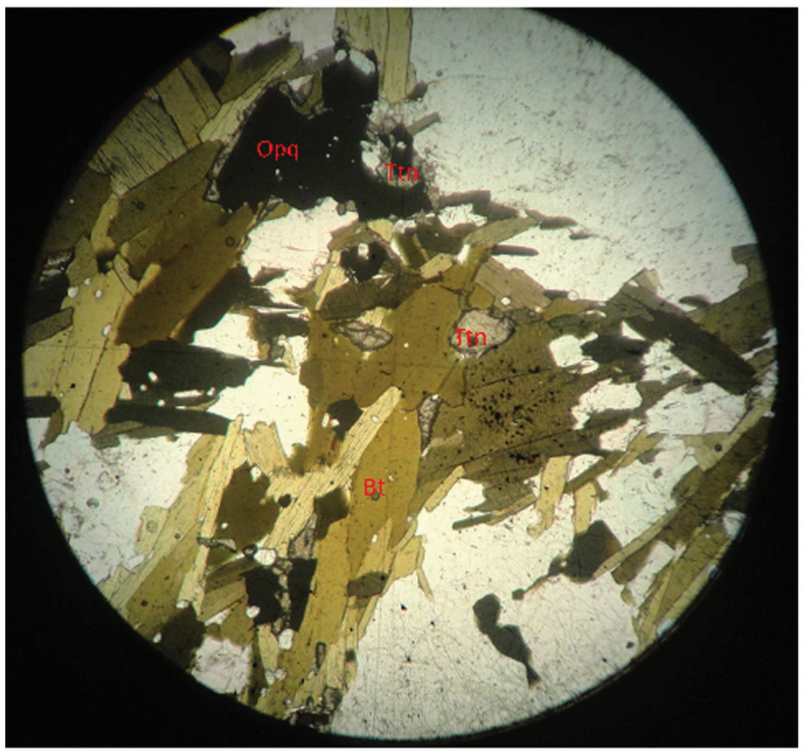

Figure 9: *Photomicrograph showing a close relationship between biotite (Bt) and titanite (Ttn). Take a note of reaction rim of titanite (Ttn) round the opaque (Opq) (PPL).*

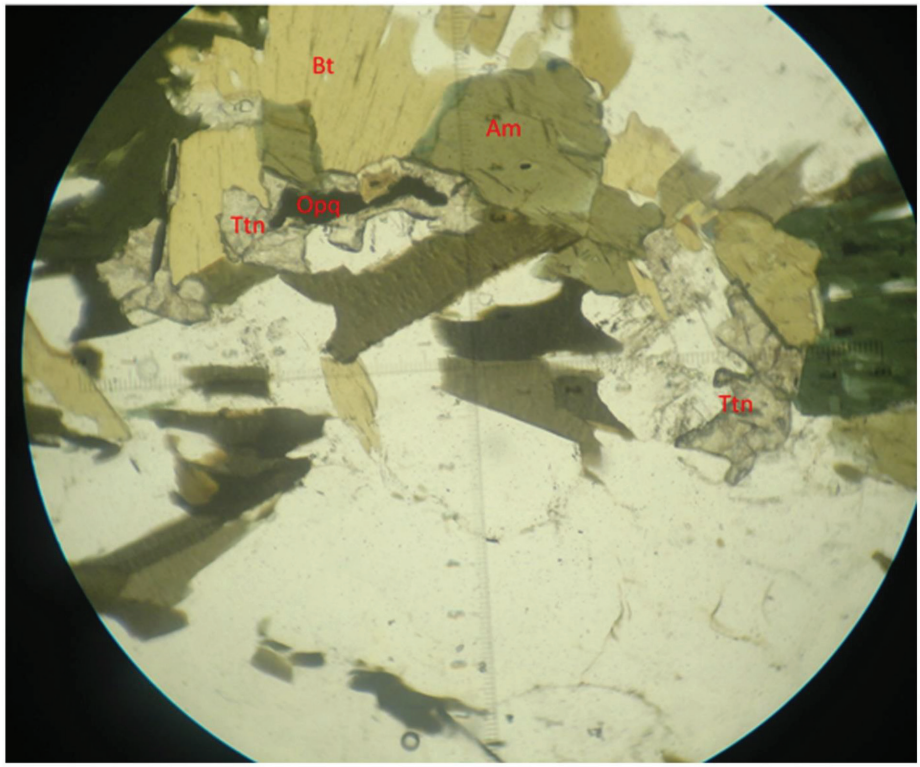

Figure 10: *Photomicrograph showing reaction rim of titanite (Ttn) on opaque (Opq) (PPL).*

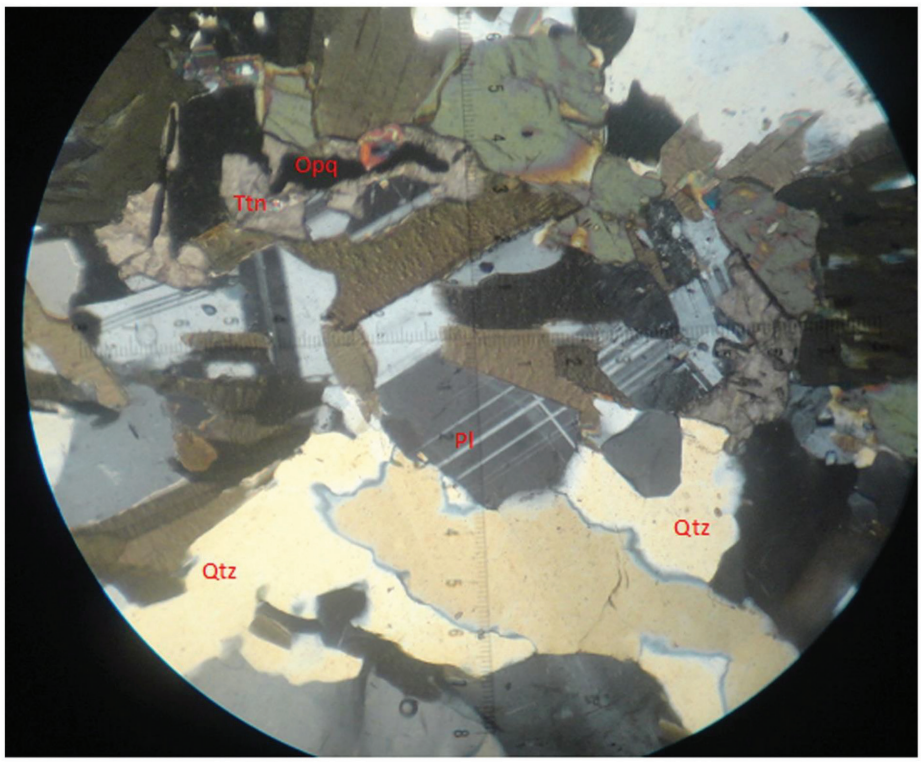

Figure 11: *Photomicrograph showing reaction rim of titanite (Ttn) on opaque (Opq) (XPL).*

to opaque mineral, a common phenomenon in granitoids indicating a late fluid activity [22]. Results from experiments suggest that titanite forms as an early phase during crystallisation of magma [23, 24]. Secondary titanite observed is anhedral and occurs as reaction rim round opaque minerals (Figures 9–11), and this reaction can be supported by the equation given below:

Plagioclase 1 (Ca-rich) + Ilmenite =>
Titanite + Plagioclase 2 (Na-rich)

The titanite grains observed show no visible form of zoning. The secondary titanite has been found to be associated with sericitisation of plagioclase and chloritization of biotite as observed in the tonalite [25]. These set of reactions represent retrogressive events probably prompted by moderate heating and fluid activity [22, 26] and can be represented by an equation such as:

Plagioclase 1 (Ca-rich) + Biotite (Ti-rich) =>
Titanite + Chlorite + Plagioclase 2 (Na-rich)

This type of alteration reaction liberates titanium that is locked within biotite [19]. In this regard, titanite can be said to be replacing early biotite and coeval with the chlorite formation (Figure 8a). The opaque mineral is likely to be ilmenite, because ilmenite is an opaque mineral with titanium in its structure. The accessory mineral assemblages such as allanite and titanite have been found to be sensitive to parameters such as temperature, oxygen fugacity, melt composition, as well as the dissolution history of evolving magma [27, 28]. The apatite which occur as inclusions in biotite can be said to have formed very early during the magmatic process because of the euhedral nature of crystals and occurrence as inclusions in biotite (Figure 6a) and, thus, can be regarded as primary igneous mineral. Plagioclase crystals observed have some of the following features: Carlsbad/albite twinning sericitisation, compositional zoning and deformed twin lamellae (Figures 8c and 8d). The sericitisation can be supported by the reaction involving plagioclase, biotite, opaque (ilmenite), muscovite, titanite and quartz [22]. Zoned plagioclase could have resulted from rapidly cooled magma leading to disequilibrium growth occurring during large undercooling. Compositional zoning in crystals is a tool in determining the magmatic history of plutonic rocks [29, 30]. The foliation observed on the outcrop and the deformation of the twin lamellae in the plagioclase is an indication that the rock has been subjected to tectonic activity. Twin lamellae of plagioclase with bent surfaces are common, an indication of syn-magmatic or post-magmatic crystallisation feature.

Conclusion

The allanite observed is found to have formed early as a result of primary crystallisation and has undergone metamictisation. Both primary and secondary titanite were observed, and the secondary titanite formed at the expense of titanite. The zoned plagioclase is an evidence that there was rapid cooling of magma close to the Earth's surface. Tonalite under study has been subjected to tectonic activities with evidence recorded on the plagioclase and the foliated nature of the rock.

References

[1] Hubbard, F.H. (1975): Precambrian crustal development in western Nigeria: indications from the Iwo region. *Geological Society of America Bulletin*, 86(4), pp. 548–554.

[2] Rahaman, M. A. (1976): Review of the basement geology of Southwestern Nigeria. In: *Geology of Nigeria*, C.A. Kogbe (ed.). Elizabethan Publishing Co.: Lagos, pp. 41–58.

[3] Poitrasson, F. (2002): In situ investigations of allanite hydrothermal alteration: examples from calc-alkaline and anorogenic granites of Corsica (southeast France). *Contributions to Mineralogy and Petrology*, 142(4), pp. 485–500.

[4] Gieré, R., Sorensen, S.S. (2004): Allanite and other REE-rich epidote-group minerals. *Reviews in Mineralogy and Geochemistry*, 56(1), pp. 431–493.

[5] Gromet, L.P., Silver, L.T. (1983): Rare earth element distributions among minerals in a granodiorite and their petrogenetic implications. *Geochimica et Cosmochimica Acta*, 47(5), pp. 925–939.

[6] Dawes, R.L., Evans, B.W. (1991): Mineralogy and geothermobarometry of magmatic epidote-bearing dikes, Front Range, Colorado. *Geological Society of America Bulletin*, 103, pp. 1017–1031.

[7] Catlos, E.J., Sorensen, S.S., Harrison, T.M. (2000): Th-Pb ion-microprobe dating of allanite. *American Mineralogist*, 85, pp. 633–648.

[8] Jiang, N. (2006): Hydrothermal alteration of chevkinite-(Ce) in the Shuiquangou syenitic intrusion, northern China. *Chemical Geology*, 227(1–2), pp. 100–112.

[9] Chen, W.T., Zhou, M.F. (2014): Ages and compositions of primary and secondary allanite from the Lala Fe–Cu deposit, SW China: implications for multiple episodes of hydrothermal events. *Contributions to Mineralogy and Petrology*, 168(2), p. 1043.

[10] Vlach, S.R., Gualda, G.A. (2007): Allanite and chevkinite in A-type granites and syenites of the Graciosa Province, southern Brazil. *Lithos*, 97(1–2), pp. 98–121.

[11] Mitropoulos, P. (1987): Primary allanite in andesitic rocks from the Poros Volcano, Greece. *Mineralogical Magazine*, 51(362), pp. 601–604.

[12] Berger, A., Rosenberg, C., Schaltegger, U. (2009): Stability and isotopic dating of monazite and allanite in partially molten rocks: examples from the Central Alps. *Swiss Journal of Geosciences*, 102(1), pp. 15–29.

[13] Barth, S., Oberli, F., Meier, M. (1989): U-Th-Pb systematics of morphologically characterized zircon and allanite: a high-resolution isotopic study of the Alpine Rensen pluton (northern Italy). *Earth Planet Sci Lett*, 95, pp. 235–254.

[14] Barth, S., Oberli, F., Meier, M. (1994): Th-Pb versus U-Pb isotope systematics in allanite from co-genetic rhyolite and granodiorite: implications for geochronology. *Earth Planet Sci Lett*, 124, pp. 149–159.

[15] Davis, D.W., Schandl, E.S., Wasteneys, H.A. (1994): U-Pb dating of mineral alteration in halos of Superior Province massive sulfide deposits: syngenesis versus metamorphism. *Contrib Mineral Petrol*, 115, pp. 427–437.

[16] Gregory, C.J., Rubatto, D., Allen, C.M., Williams, I.S., Hermann, J., Ireland, T. (2007): Allanite micro-geochronology: a LA-ICP-MS and SHRIMP U–Th–Pb study. *Chemical Geology*, 245(3–4), pp. 162–182.

[17] Darling, J.R., Storey, C.D., Engi, M. (2012): Allanite U–Th–Pb geochronology by laser ablation ICPMS. *Chemical Geology*, 292, pp. 103–115.

[18] McFarlane, C. R. (2016): Allanite UPb geochronology by 193 nm LA ICP-MS using NIST610 glass for external calibration. *Chemical Geology*, 438, pp. 91–102.

[19] Rimsaite, J. (1982): Alteration of Radioactive Minerals in Granite and Related Secondary Uranium Mineralizations. In: *Ore Genesis.* Springer: Berlin, Heidelberg, pp. 269–280.

[20] Janeczek, J., Eby, R.K. (1993): Annealing of radiation damage in allanite and gadolinite. *Physics and Chemistry of Minerals*, 19(6), pp. 343–356.

[21] Wood, S.A., Ricketts, A. (2000): Allanite-(Ce) from the Eocene Casto granite, Idaho: response to hydrothermal alteration. *The Canadian Mineralogist*, 38(1), pp. 81–100.

[22] Broska, I., Harlov, D., Tropper, P., Siman, P. (2007): Formation of magmatic titanite and titanite–ilmenite phase relations during granite alteration in the Tribeč Mountains, Western Carpathians, Slovakia. *Lithos*, 95(1–2), pp. 58–71.

[23] Watson, E.B., Harrison, T.M. (1984): Accessory minerals and the geochemical evolution of crustal magmatic systems: a summary and prospectus of experimental approaches. *Phys. Earth Planet. Int.*, 1984, 35, pp. 19–30.

[24] Xirouchakis, D., Lindsley, D.H. (1998): Equilibria among titanite, hedenbergite, fayalite, quartz, ilmenite, and magnetite: experiments and internally consistent thermodynamic data for titanite. *Am. Mineral.,* 83, pp. 712–749.

[25] Putnis, A. (2002): Mineral replacement reactions: from macroscopic observation to microscopic mechanism. *Mineral. Mag*. 66, pp. 689–708.

[26] Corfu, F., Stone, D. (1998): The significance of titanite and apatite U–Pb ages: constraints for the post-magmatic thermal-hydrothermal evolution of a batholithic complex, Berens River area, northwestern Superior Province, Canada. *Geochim. Cosmochim. Acta,* 62, pp. 2979–2995.

[27] Paterson, B. A., Stephens, W. E., Herd, D. A. (1989): Zoning in granitoid accessory minerals as revealed by backscattered electron imagery. *Mineral. Mag.,* 53, pp. 55–61.

[28] Wones, D.R. (1989): Significance of the assemblage titanite + magnetite quartz in granitic rocks. *Am. Mineral.,* 74, pp. 744–749.

[29] Loomis, T.P. (1981): An investigation of disequilibrium growth processes of plagioclase in the system anorthite-albite-water by methods of numerical simulation. *Contributions to Mineralogy and Petrology*, 76(2), pp. 196–205.

[30] Loomis, T.P., Welber, P.W. (1982): Crystallization processes in the Rocky Hill granodiorite pluton, California: an interpretation based on compositional zoning of plagioclase. *Contributions to Mineralogy and Petrology*, 81(3), pp. 230–239.

Instructions for Authors

About the Journal

RMZ – Materials and Geoenvironment (RMZ – Materiali in geookolje) is a periodical publication with four issues per year. It was established in 1952 and renamed to RMZ – M&G in 1998). The main topics of Journal are Mining, Geotechnology, Metallurgy, Materials, Geology and Geoenvironment.
RMZ – M&G publishes original scientific papers, review papers, preliminary notes and professional papers in English. Only professional papers will exceptionally be published in Slovene. In addition, evaluations of other publications (books, monographs, etc.), in memoriam, presentation of a scientific or a professional event, short communications, professional remarks and reviews published in RMZ – M&G can be written in English or Slovene. These contributions should be short and clear.

- *Original scientific papers* represent unpublished results of original research.
- *Review papers* summarize previously published scientific, research and/or expertise articles on a new scientific level and can contain other cited sources which are not mainly the result of the author(s).
- *Preliminary notes* represent preliminary research findings, which should be published rapidly (up to 7 pages).
- *Professional papers* are the result of technological research achievements, application research results and information on achievements in practice and industry.
- *Publication notes* contain the author's opinion on newly published books, monographs, textbooks, etc. (up to 2 pages). A figure of the cover page is expected, as well as a short citation of basic data.
- *In memoriam* (up to 2 pages), a photo is expected.
- *Discussion of papers* (Comments) where only professional disagreements of the articles published in previous issue of RMZ – M&G can be discussed. Normally the source author(s) reply to the remarks in the same issue.
- *Event notes* in which descriptions of an scientific or a professional event are given (up to 2 pages).

Form of the Manuscript

Basic Requirements for Manuscript

- Optimal number of pages is 7 to 15; longer articles should be discussed with the Editor-in-Chief prior to submission.
- Text of the manuscript should be written in Times New Roman font with 12-point size and 1.5 line spacing.
- Figures, tables and formulas should be included in the text of the manuscript.
- Headings should be written in Arial bold font (12-point size) and should not be numbered.
- Subheadings should be written in Arial italic font (12-point size).
- The electronic version of the manuscript should be simple, without complex formatting. For highlighting, only bold and italic types should be used.
- The manuscript should be submitted in Microsoft Word via the online system.

Composition of the Manuscript

The manuscript should have the following composition:

Title

The title of the article should be precise, informative and not longer than 100 characters. The author should also indicate the short version of the title. The title should be written in English and for Slovenian authors also in Slovene.

Author's Information
Author's information should include name and surname of the authors, the address of the institution and the e-mail address of the corresponding author.

Abstract
An Abstract presents the purpose of the article and the main results and conclusions. It should not exceed 180 words. It should be written in English and for Slovenian authors also in Slovene.

Keywords
A list of up to 5 key words (3 to 5) that will be useful for indexing or searching. They should be written in English and for Slovenian authors also in Slovene.

Introduction
An Introduction should provide a review of recent literature and sufficient background information to allow the results of the article to be understood and evaluated.

Materials and methods
The Materials and method section details the theoretical or experimental methods and materials used to obtain the results.

Results and discussion
The result section should clearly and concisely present the data, using figures and tables where appropriate. The Discussion section should describe the relationships shown by results and discuss the significance of the results, making comparison with previously published work.

Conclusions
A Conclusions section should present one or more conclusions that have been made from the results and discussion.

Acknowledgements
Acknowledgement (optional) of collaboration or preparation assistance may be included. If the research was funded, please note the source of funding.

References
A references section includes a list of references, which comprises all the references cited in the text.

Units and Abbreviations

Only standard SI symbols and abbreviations should be used in the text, tables and figures. Symbols for physical quantities in the text should be written in italics (e.g. m, l, v, T). Symbols for units that consist of letters should be in plain text with spaces after number (e.g. 10 m, 5.2 kg/s, 2 s^{-1}, 50 kPa). All abbreviations should be spelt out in full on first appearance. A period/full stop is used as the decimal point (3.14 and not 3,14).

Figures

Figures must be cited in consecutive numerical order in the text and referred to in both the text and the captions as Figure 1, Figure 2, etc. Figures should be originals, made in an electronic form (Microsoft Excel, Adobe Illustrator, Inkscape, AutoCAD, CorelDraw, etc.) and saved in .eps, .tiff or .jpg format with a resolution of at least 300 dpi. The width of the figures should be at least 152 mm. Figures should be named the same as in the article (Figure 1, Figure 2, etc.). Letters and numbers should be readable, with equal sizes and fonts in all figures.
Figures should also be submitted as a separate document, i.e. separated from the text in the article.

Tables

Tables must be cited in consecutive numerical order in the text and referred to in both the text and the caption as Table 1, Table 2, etc. Tables should be prepared using a table editor and not inserted as a graphic.

Equations

Equations should be numbered in consecutive numerical order with the use of round brackets on its right side and referred in the text as Equation (1), Equation (2), etc. The equations should be written using equation editor.

References

The references should be cited in the same order as they appear in the article. Where possible the DOI for the reference should be included at the end of the reference. They should be numbered in square brackets. Any references cited in the article must be given in full. Unpublished results and personal communications are not recommended in the reference list, but may be mentioned in the text, if necessary. Please use examples in Appendix as a guide.

Manuscript Submission

Please submit your article via RMZ – M&G Editorial Manager System. You can find it on the address
http://edmgr.editool.com/rmzmag/default.htm
Log in as an author and submit your article. Note that the manuscript should be submitted in Microsoft Word format. High resolution figures should be included in the text and also submitted as a separate document.
You can follow the status of your submission in the Editorial Manager System and your e-mail.

Review Process

All manuscripts will be supervised in a review process. The reviewers evaluate the manuscript and can ask the authors to change particular segments, and propose to the Editor-in-Chief the acceptability of the submitted articles. Authors are requested to identify three reviewers and may also exclude specific individuals from reviewing their manuscript. The Editor-in-Chief has the right to choose other reviewers. The name of the reviewer remains anonymous. The technical corrections will also be done and the authors can be asked to correct the missing items. The final decision on the publication of the manuscript is made by the Editor-in-Chief.

Production Process

After composing PDF document and language editing, author receive document for proofreading. If author have any comments, mark them and write a comment in the same PDF document. Comments in another document or scanned and corrected document are inappropriate. Upload PDF document in Editorial Manager System under the different name.

If author do not cooperate in production process, manuscript can be rejected, despite of receiving letter of acceptance.

Appendix: citing of references

Journal article:

Surname 1, Initials, Surname 2, Initials (year): Title. *Journal*, volume(number), page range, DOI code. Journal title should be complete and not abbreviated. Note that *Journal Title* is italicized.

[1] Malej, S., Terčelj, M., Peruš, I., Kugler, G. (2016): Influence of cooling mode in relation to casting and extrusion parameters on mechanical properties of AA6082. *Materials and Geoenvironment*, 64(1), pp. 11–19, DOI:10.1515/rmzmag-2016-0022.

Book:

Surname 1, Initials, Surname 2, Initials (year): *Title*. Publisher: place of publication, number of pages. Note that the *Title of the book* is italicized.

[2] Reynolds, J.M. (2011): *An introduction to applied and environmental geophysics*. Wiley-Blackwell: Chichester, 710 p.

Chapter in an Edited Book:

Surname 1, Initials, Surname 2, Initials (year): Chapter title. In: *Book title*, Editor Surname 1, Initials, Editor Surname 2, Initials (ed(s).). Publisher: place of publication, page range. Note that the *Book title* is italicized.

[3] Blindow, N., Eisenburger, D., Illich, B., Petzold, H., Richer, T. (2007): Ground Penetrating Radar. In: *Environmental Geology – Handbook of Field Methods and Case Studies, Knödel*, K., Lange, G., Voigt, H.J. (eds.). Springer: Berlin, pp. 283–335.

Proceeding Paper:

Surname 1, Initials, Surname 2, Initials (year): Paper title. In: *Proceedings title*, place of symposium/conference, Editor Surname 1, Initials, Editor Surname 2, Initials (ed(s).). Publisher: place of publication, page range. Note that the *Proceedings title* is italicized.

[4] Benac, Č., Gržančić, Ž., Šišić, S., Ružić, I. (2008): Submerged Karst Phenomena in the Kvarner Area. In: *Proceedings of the 5th International ProGEO Symposium on Conversation of the Geological Heritage*, Rab, Croatia, Marjanac, T. (ed.). Pro GEO Croatia: Zagreb, pp. 12–13.

Master Thesis or Ph. D. Thesis:

Surname, Initials (year): *Title*. Type of document (Master Thesis or Ph. D. Thesis). Publisher: place of publication, number of pages. Note that the *Title* is italicized.

[5] Rošer, J. (2010): *Study of the effects of sediments on seismic ground motion in the city of Ljubljana using the microtremor survey method*. Ph. D. Thesis. University of Ljubljana, Faculty of Natural Sciences and Engineering, Department of Geotechnology, Mining and Environment: Ljubljana, 278 p.

Standard:

Standard-Code (year). *Title of the Standard*. Organisation: place. Note that the *Title of the Standard* is italicized.

[6] ISO/ICS 17892-10:2018. *Geotechnical investigation and testing – Laboratory testing of soils – Part 10: Direct shear tests*. International Organization for Standardization: Genova.

Electronic source:

Title [online]. Surname, Initials or Company name, renewed (date) [cited (date)]. Available on: *http://address*. Note that the *www address* is italicized.

[7] CASREACT – Chemical reactions database [online]. Chemical Abstracts Service, renewed 2/15/2000 [cited 2/25/2000]. Available on: *http://www.cas.org/casreact.html*.

These instructions are valid from February 2020.